Universidade de Aveiro
2023

Francisco Rodrigues Marques

Acoustic analysis of new sustainable materials for heat pump structural solutions

Análise acústica de novos materiais sustentáveis para soluções estruturais de bombas de calor

Universidade de Aveiro
2023

Francisco Rodrigues Marques

Acoustic analysis of new sustainable materials for heat pump structural solutions

Análise acústica de novos materiais sustentáveis para soluções estruturais de bombas de calor

Relatório de Estágio apresentado à Universidade de Aveiro para cumprimento dos requisitos necessários à obtenção do grau de Mestre em Engenharia Mecânica, realizado sob orientação científica do Professor Doutor Rui António da Silva Moreira, Professor Auxiliar do Departamento de Engenharia Mecânica da Universidade de Aveiro, e da Doutora Idalina Alcântara Pinto Martins, Engenheira Acústica da Bosch Home Comfort S.A..

O júri / The jury

Presidente / President   **Prof. Doutor Sérgio Manuel Oliveira Tavares**
Professor Auxiliar em Regime Laboral da Universidade de Aveiro

Vogais / Committee   **Prof. Doutor José Fernando Dias Rodrigues**
Professor Associado da Faculdade de Engenharia da Universidade do Porto

Prof. Doutor Rui António da Silva Moreira
Professor Auxiliar da Universidade de Aveiro

**Agradecimentos /
Acknowledgements**

Abstract

This work aims to identify the most effective materials for sound insulation in heat pumps, incorporating improvements in the testing procedure. The study focuses on the evaluation of bonded foam (provided by the company Flexicel) and geopolymer samples, utilizing both manual and automatic measurement methods. To enhance the testing process, a sample holder capable of measuring samples with various thicknesses and components for the correct fixation of the intensity probe were developed. A 3D printer was used has the basis for the automatic system and additionally G-Code commands were written to establish an automated scanning pattern. Through Scan & Paint measurements, the sound intensity for each frequency of each sample was obtained, and the pressure-intensity method was employed to calculate the sound transmission loss. The Scan & Paint technique was also used to assess the uniformity of sound fields, spatial distribution of sound intensity and potential sound leaks in order to gain comprehensive insight into the performance of the materials and ways to improve the testing conditions for each individual sample. Results highlight a low density coloured bonded foam with bitumen heavy layer exhibiting superior sound insulation capabilities among the bonded foam samples, followed by a polyurethane (PUR) foam with heavy layer as well. For these samples, sound transmission loss surpassed 30 dB from 2000 Hz onwards and revealed good results in the rest of the frequency range. Coloured foam sound transmission loss peaked at 5000 Hz with 41.5 dB. Moreover, the geopolymer samples, specifically those with 30 mm and 40 mm thickness, demonstrated promising sound transmission loss results. Evaluating results from both manual and automatic tests, it was proved that samples with a lower content of aluminium (0.10%) and bigger thickness provided overall better acoustic performances, presenting a peak of around 36.7 dB at 4000 Hz and also interesting results in lower frequencies. Surprisingly, the geopolymer sample that showed the highest sound transmission loss value was the one with 0.15% aluminium and thickness of 30 mm, presenting 36.8 dB at 4000 Hz. Notably, the integration of the automated scanning method improved the efficiency and accuracy of the testing procedure. However, significant disparities in sound transmission loss values were observed between the manual and automatic measurement methods, specially in geopolymer samples, although they were not nearly as pronounced in the bonded foam samples. Consequently, caution is warranted when interpreting the results obtained through the automated measurements, as it is suggested that the manual tests provide a more reliable basis for evaluating the sound insulation properties of the materials.

Palavras-chave   Bomba de calor; Câmara anecoica; Câmara reverberante; Intensidade sonora; Materiais sustentáveis; Scan & Paint; Transmissão sonora

Resumo   Este trabalho tem como objetivo identificar os materiais mais eficazes para isolamento acústico de bombas de calor, incorporando melhorias no procedimento de ensaio. O estudo centra-se na avaliação de amostras de aglomerados de espumas (fornecidas pela empresa Flexicel) e de geopolímeros, utilizando métodos de medição manuais e automáticos. Para melhorar o processo de ensaio, foram desenvolvidos um suporte de amostras capaz de medir amostras com várias espessuras e componentes para a correcta fixação da sonda de intensidade. Foi utilizada uma impressora 3D como base para o sistema automático e, adicionalmente, foram escritos comandos em código G para estabelecer um padrão de varrimento automatizado. Através das medições utilizando a técnica Scan & Paint, obteve-se a intensidade sonora para cada frequência de cada amostra e utilizou-se o método de pressão-intensidade para calcular a perda de transmissão sonora. A técnica Scan & Paint foi também utilizada para avaliar a uniformidade dos campos sonoros, a distribuição espacial da intensidade sonora e as potenciais fugas de som, de modo a obter uma visão abrangente do desempenho dos materiais e de formas de melhorar as condições de teste para cada amostra individualmente. Os resultados destacam uma espuma colorida de baixa densidade com camada dura de betume que apresenta capacidades superiores de isolamento sonoro entre as amostras de aglomerados de espumas, seguida de uma espuma de poliuretano (PUR) também com camada dura. Para estas amostras, a perda de transmissão sonora ultrapassou os 30 dB a partir dos 2000 Hz e revelou bons resultados no resto da gama de frequências. A perda de transmissão sonora da espuma colorida atingiu o pico a 5000 Hz com 41.5 dB. Para além disso, as amostras de geopolímeros, especificamente aquelas com 30 mm e 40 mm de espessura, demonstraram resultados promissores de perda de transmissão sonora. Em termos globais, avaliando os resultados dos ensaios manuais e automáticos, verificou-se que as amostras com menor conteúdo de alumínio (0,10%) e maior espessura proporcionaram melhores desempenhos acústicos, apresentando um pico de cerca de 36.7 dB nos 4000 Hz e também resultados interessantes em frequências mais baixas. Surpreendentemente, o geopolímero que apresentou o valor mais elevado de perda de transmissão sonora continha 0.15% de conteúdo de alumínio e uma espessura de 30 mm, apresentando 36.8 dB a 4000 Hz. É de salientar que a integração do método de varrimento automático melhorou a eficiência e a precisão do procedimento de ensaio. No entanto, foram observadas disparidades significativas nos valores de perda de transmissão sonora entre os métodos de medição manual e automático, especialmente nas amostras de geopolímeros, embora não tenham sido tão acentuadas nos aglomerados de espuma. Consequentemente, é necessária alguma precaução ao interpretar os resultados obtidos através das medições automáticas, uma vez que se sugere que os testes manuais fornecem uma base mais fiável para avaliar as propriedades de isolamento acústico dos materiais.

Contents

List of Tables

Intentionally blank page.

List of Figures

List of Abbreviations

EU   European Norm

FE   Finite Elements

GFC   Geopolymer Foam Concrete

HL   Heavy Layer

ISO   International Organization for Standardization

MDF   Medium Density Fiberboard

PUR   Polyurethane

RWF   Rock Wool Fiber

SEA   Statistical Energy Analysis

SPL   Sound Pressure Level

STL   Sound Transmission Loss

WPC   Wood Plastic Composites

Intentionally blank page.

Chapter 1

Introduction

In this chapter an introduction of the work is made which includes a contextualization and the main objective of the work. A brief description of the work plan is also given, as well as some basic ideas about noise and heat pumps. All the work was carried out on the premises of Bosch Home Comfort S.A., in particular in the sound laboratory.

1.1 Bosch Home Comfort S.A.

Bosch Home Comfort S.A. started its activity in 1988 and is one of the main companies driving the economy of the city of Aveiro. Currently, Bosch Home Comfort S.A. (Figure 1.1) focuses on offering efficient solutions for room climate, domestic hot water and decentralised energy management, working on water heaters, boilers, electrical appliances for water heating and heat pumps, as well as in the development and design of new products and devices. The company offers these new solutions taking into consideration market needs and maintaining a constant focus on new ways to reduce CO_2 emissions, due to environmental concerns of the modern society.

It is important to note that the acoustic testing system to be used in this work was developed in previous works and is available at the company's facilities.

Figure 1.1: Bosch Home Comfort, Aveiro [1].

1.2 Background

Bosch Home Comfort S.A. is developing a new modular concept for residential heat pumps. This research effort has its origin in two major market requirements: acoustic emission of the equipment (imposed by the gradual and growing legal restriction at this level, combined with the growing demand for this type of equipment for the residential sector) and the need to reduce the use of materials of non-renewable origin and reduce the ecological footprint of the materials and manufacturing technologies used in the production of this equipment, as well as reducing the impact of this equipment at its end of life. This research and development work includes 3 lines of research:

1. Replacement of structural and acoustic insulation elements by functionally equivalent elements in materials of renewable origin or reused materials.

2. Design of a modular concept, separating the evaporator and ventilator assembly from the compressor and the refrigerant circuit.

3. Optimisation of the operation controller to ensure efficient and intelligent management combining the needs of the consumer, the availability of the electrical network and the legal limits imposed at acoustic level.

The works that were previously developed focused on the construction and validation of a small scale reverberant chamber, confirming its applicability in terms of frequency ranges, sound levels and sample sizes. However, the procedure is limited in some aspects, mainly concerning the sound transmission measurement system with the aid of a probe, since it was manually executed and therefore does not guarantee the repeatability and homogeneity of the results, since the human factor has to be taken into account. The veracity of the results obtained may also be called into question as a result of the new setup carried out to serve as the testing system, characterised by a reverberation chamber placed inside a hemi-anechoic chamber, due to the relative dimensions between chambers, the relationship between chamber volume and the size of the analysis frequency range panel. Although promising, some adjustments regarding the testing system are required. Therefore, a further validation of the results obtained as a result of the use of the system and even of the assembly that characterises it may serve as a basis for future work concerning acoustic measurement techniques, as well as for a possible standardisation of a testing setup to be carried out by the industry.

1.3 Heat Pumps

With growing environmental concern, a transition to environmentally friendly systems is essential. There is an increasing demand for energy-efficient and cost-effective space heating and cooling applications. In this context, heat pumps have been identified as a key technology and the global market for these devices is expected to grow at an annual rate of 8.1%, reaching USD 136.8 billion in terms of revenue by 2030 [2].
Heating and cooling account for 30% of CO_2 emissions in commercial settings, increasing to 38% for residential and water heating alone, represents 15% of CO_2 emissions in the residential sector [3]. Carbon dioxide emissions from operating a heat pump are directly linked to the carbon content of the electricity used to power it and some studies even show

that CO_2 emissions from domestic heating are reduced by around 50% when replacing oil, solid fuel or electric heating [4].

Heat pumps can be divided in four major groups [5]:

1. Air Source Heat Pumps - These can be installed inside or outside the house. There are also split systems with an indoor unit and an outdoor unit.

2. Ground Source Heat Pumps - Copper or plastic tubes are buried underground, working as heat exchangers. Ground source heat pumps extract heat from the ground either by a vertical or horizontal collector.

3. Water Source Heat Pumps - The heat is extracted from the water and since water is an excellent energy carrier, these heat pumps are normally quite efficient.

4. Electrically and Thermally Driven Heat Pumps - In electrically driven heat pumps the compression cycle is driven by electricity, while in thermally driven heat pumps, normally an engine is used for that purpose.

1.3.1 Working principal

Heat pumps transfer heat rather than converting it from a fuel like combustion heating system. Therefore, the operation principal of a heat pump is the transfer of thermal energy in the form of heat against its natural gradient, from a cold place to a hotter one. This exchange occurs through a liquid refrigerant that needs to be warmed up in order to transfer its energy to the domestic water circuit.

Figure 1.2 shows a schematic diagram of a heat pump system. The four main components present in a heat pump are an evaporator, a compressor, an internal heat exchanger and an expansion valve. Firstly, an axial or centrifugal fan draws cold ambient air through the evaporator, absorbing the energy and transferring it to the refrigerant circuit via forced convection. Since the refrigerant can evaporate at low temperatures, it undergoes a phase transition from fluid to gas. The compressor compresses the gaseous refrigerant, rising its temperature and then the internal heat exchanger allows the high pressure gas to transfer its energy to the heating circuit inside the house. Finally, the temperature of the refrigerant drops, which is now in a liquid state again as a result of condensation during the heat exchange, and goes through an expansion vale which lowers the pressure and temperature. Initial conditions are then restored [6].
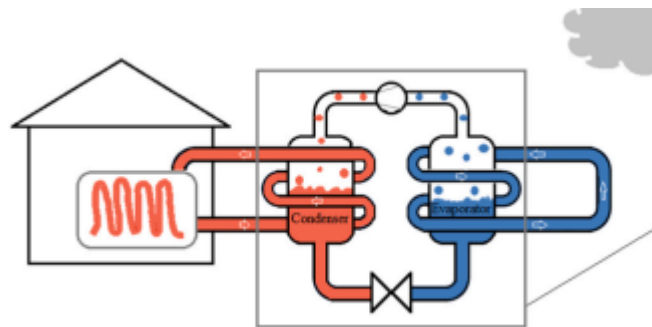
Figure 1.2: Heat pump working principle diagram [7].

1.3.2   Heat Pump Noise

Heat pump acoustic emissions and vibrational energy are categorized in three forms [6]:

- Airborne noise - Acoustic radiation from the source and the nearby structures, propagating in the surrounding air. It is measured using microphones or sound intensity probes.

- Hydraulic or fluid-borne noise - Originates in the pressure pulses emitted by the source in the liquid columns of the system and which are mainly responsible for noise emissions of the piping.

- Structure-borne noise - This noise is generally due to dynamic forces by the components and are evaluated through force sensors and accelerometers.

Residential heat pumps can generate some noise, with users saying intrusive noise is a problem, especially in Air Source Heat Pumps [7].

Since 1980, the World Health Organization has addressed the problem of community noise, ranging from construction and industries to home appliances and machinery [8]. Exposure to unwanted levels of noise can lead to several problems such as tinnitus, increased stress, sleep problems and even heart diseases. The organization listed noise pollution as the second most hazardous environmental factor in Europe and defined some guidelines in order to reduce its impact on people's daily lives.

The main components of heat pumps in terms of noise generation are the compressor and the fan, with slight noise also provided by the expansion valve or electrical transformers in the system. In general, these are the components that require acoustic treatment most of the time [9].

There are regulations addressing the standards for heat pumps, namely through the standard EN 12102 that sets the requirements for the determination of levels of emitted sound power in heat pumps and other similar devices. This can be achieved by means of acoustic pressure and acoustic intensity techniques, as well as through vibration measurements [10]. To reduce the level of noise emitted by heat pumps these appliances are often covered by a metal or plastic case with some form of acoustic isolation (using polymeric foams, stone or glass wool).

1.4   Objective

The goal of the work is to develop an analysis on sound transmission regarding materials for heat pump construction, being of interest the study of several sustainable materials. These include geopolymers and bonded or rebonded foam, which are recycled materials obtained from the remains of different kinds of foams than can have different colours, densities and properties. Sound transmission loss measurements using the sound intensity method is to be used.

The major guidelines for these tests are clear, even though the test setup is considered an adaptation of the main procedure for laboratory measurements and so it was adjusted accordingly.

The first objective is to optimize the setup to overcome some existing limitations, namely regarding the lack of flexibility for testing samples of different thicknesses and also of an automatic system for scanning the sample plane to capture the values of sound intensity.

Developing an improved sample holder and an automatic system for measuring purposes would help to test different sustainable materials and combinations, guaranteeing the homogeneity and repeatability of the test procedure, as opposed to manual measurements.
Secondly, there is a need to evaluate the reliability of the automatic system for these type of studies, comparing it to the manually performed tests. Finally, the material with the best acoustic performance is to be carefully selected to then be considered a good solution for sound insulation in heat pump systems.

1.5   Work outline

This work begins with a presentation of concepts regarding the different tests and materials considered in the acoustic domain, followed by brief theoretical concepts, in Chapter 2 and Chapter 3, respectively.
Chapter 4 discusses the improvements made in the experimental procedure and Chapter 5 focuses on the materials selected for testing, their properties and how the tests themselves were performed.
The results are presented in detail in Chapter 6, taking into account several variables such as the grouping of the materials considering their composition, the comparison of test methods and the evaluation of the best materials for soundproofing to be considered for heat pump solutions.
At last, Chapter 7 presents the main conclusions drawn throughout the work and how this topic can be further developed in future studies.

Intentionally blank page.

Chapter 2

State of the Art

This chapter presents the methods for sound transmission loss measurements, as well as an overview of Scan & Paint technology for acoustic research. A few studies are also presented regarding the use of sustainable materials for noise reduction applications, notably foams, geopolymers and materials containing natural particles.

2.1 Sound transmission measuring methods

Techniques for determining sound transmission loss include the impedance tube method and the two-chamber method, the latter being the focus of this work. There can be defined three major configurations within the two-chamber method:

1. Two reverberation chambers.

2. Reverberation and anechoic chambers.

3. Two small scale reverberation chambers.

Regarding the two-chamber method, a difference is also established according to the configurations defined by the standards taking into account the parameters used to assess sound transmission loss, which are sound intensity and sound pressure. In the configuration with one reverberation chamber and one anechoic chamber, both sound pressure and intensity are considered, whereas in the two reverberation chambers setup, only sound pressure is considered.

2.1.1 Impedance tube

An impedance tube (Figure 2.1) is used for acoustic characterisation of materials, especially for small samples. It consists in placing a sample in the centre of a soundproof steel tube between microphones. Microphones will receive sound waves, which are normal to the sample, coming from a sound source placed at the end of the tube. The tests can be performed in two ways: with two loading conditions or by changing the location of the sound source among the various tests to be performed [11]. This method has been used to measure sound transmission loss of several materials, from polypropylene [12] to aluminum based, silica fume based, foam concrete and lightweight composite geopolymers. Cork samples have also been tested with impedance tubes, namely their sound absorption coefficients, following the protocol defined in EN ISO 10534-2 [13].

However, this work avoids this technique due to the lack of an impedance tube and because the size of the sample used in these tubes and the heterogeneity of the samples to be studied may be outside the limits of the homogeneity required for these tests (in particular some sandwich samples that are herein considered).
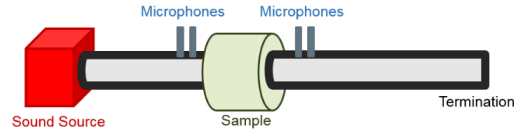
Figure 2.1: Schematic representation of an impedance tube [11].

2.1.2 Reverberation chambers

Reverberation chambers are designed to create a diffuse sound field, where sound pressure is essentially the same at every point in the chamber. Therefore, it is considered only the sound pressure. The two reverberation chamber method (Figure 2.2) involves placing microphones both in the receiving chamber and in the chamber where the sound source is placed, commonly referred as the source room, in an attempt to calculate an average for the sound pressure in the two chambers and to obtain the sound transmission loss value based on the pressure difference between the two chambers [11]. The sound transmission loss can be obtained using

$$STL = L_1 - L_2 + 10\log(\frac{S}{A}) \quad (\text{dB}) \tag{2.1}$$

where L_1 and L_2 are the average sound pressure level of the source and receiving chamber, respectively, S is the sample area and A is the equivalent sound absorption, which in turn can be calculated using

$$A = 0.16\frac{V}{T}. \tag{2.2}$$

Here, V represents the receiving chamber's volume, while T represents its reverberation time, which is the time required for a sound to fade away to a level 60 dB below its original level. The standard that defines the procedure for laboratory measurements of sound insulation is the ISO 10140-1:2021 [14].
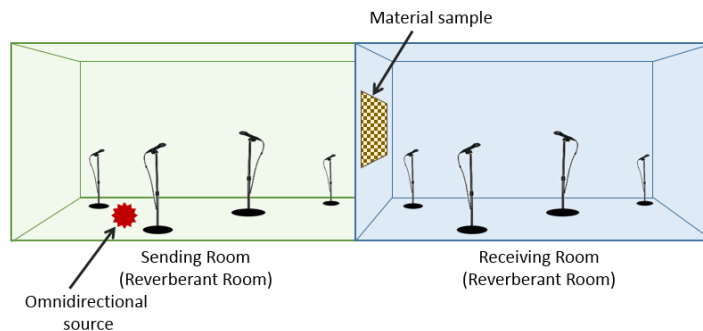
Figure 2.2: Two reverberation chamber method [11].

2.1.3   Reverberation and anechoic chambers

Contrary to a reverberation chamber, an anechoic chamber is designed to stop sound reflection and the sound absorption coefficient of its walls are approximately 1. This enables the creation of free field conditions, being very useful in acoustic measurements. In this configuration (Figure 2.3), both sound pressure and sound intensity are considered. A sound source is placed in the reverberation chamber, creating a diffuse sound field. An intensity probe is placed in the anechoic chamber to capture the sound intensity value. The sound transmission loss can be obtained using

$$STL = Lp_i - Li_t + 10\log(\frac{S_i}{S_t}) - 6.18 \quad \text{(dB)} \tag{2.3}$$

where Lp_i represents the incident sound pressure and Li_t represents the sound intensity measured in the anechoic chamber. S_i is the area incident, S_t is the area transmitted, while the constant 6.18 accounts for factors such as air density and speed of sound [11]. For many applications, it is used a hemi-anechoic chamber, which provides essentially the same features as an anechoic chamber, except the floor is not isolated and so it does not absorb sound like the rest of the walls. The ISO 15186 standard defines the method for measuring sound intensity in a hemi-anechoic chamber in order to obtain sound transmission loss values [15, 16].

The setup with an anechoic chamber has been used in numerical prediction and experimental validation of sound transmission loss in sandwich panels of composite materials [17], as well as of other materials, only changing slightly the equation to obtain the sound transmission loss and the experimental procedure, with a variation on the number of microphones and the sound sources [18].
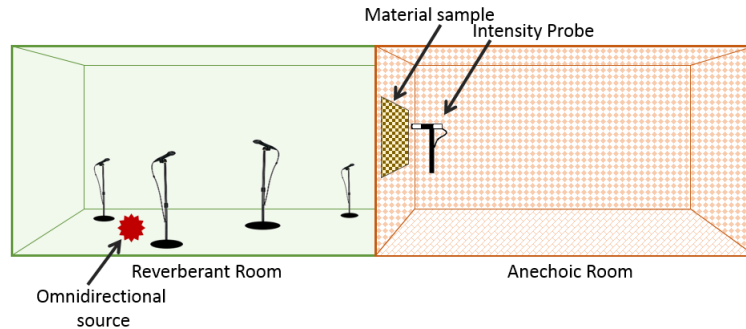
Figure 2.3: Reverberation and anechoic chamber method [11].

2.1.4   Small scale reverberation chambers

In order to perform sound measurements regarding according to the ISO standard, some specifications are necessary in terms of chamber dimensions. According to the ISO 10140-1:2021, a sample area of at least 10 m^2 is required and many times the high cost of this type of laboratory and the large amount of material required represents a major handicap. Because of this, small scale reverberation chambers are designed in order to perform the tests and are quite common in acoustic studies. These chambers reproduce the geometry of standard transmission chambers to scale [19].

Given the reduced size of the chambers, for the validation of the results a comparative study should be done based on obtained sound reduction index values. This can be achieved through tests in chambers that comply with the ISO standards established for measurements, as well as on theoretical values obtained from a simulation software that is able to predict acoustic insulation models. If the values are similar, the results can be taken as valid. Therefore, an effort should be made in the construction of the chambers, so that the geometry is as identical as possible to the standardised one and that the dimensions are consistent in terms of proportional reduction. Materials such as green composites and sheep wool have been subject to sound insulation studies using small scale chambers (Figure 2.4a) with great success [19], even though results were only considered valid from 630 Hz upwards, as cutoff frequency was considered the most limiting factor. Sound transmission loss tests of fiber panels have also been performed with small scale reverberation chambers (Figure 2.4b), through sound pressure measurements both in the source and receiving chambers [20].

(a) Small scale reverberation chambers [19].

(b) Small scale reverberation chambers for testing fiber panels [20].

Figure 2.4: Small scale reverberation chambers studies.

2.1.5 Other configurations

This subsection presents two studies based on the method using reverberation and anechoic chambers. The setup in these studies used a small scale reverberation chamber inside either a regular hemi-anechoic or an anechoic chamber.

The first one (Figure 2.5) revealed the importance of obtaining a diffuse sound field to validate the results that directly depends on the chamber characteristics, such as defining a cut-off frequency based on Schroeder's equation:

$$Fsch = 2000\sqrt{\frac{T}{V}} \quad \text{(Hz)}. \tag{2.4}$$

In this case, T represents the reverberation time and V the chamber volume. For small rooms, the modal behaviour is dominant up to frequencies higher than those observed for large rooms. To achieve a diffuse sound field inside the reverberation chamber it is imperative for absorption at the walls to be as low as possible, in order to minimize energy loss. The setup is based on the measurement of sound transmission loss using sound intensity. White noise is emitted in the reverberation chamber and the sound pressure is measured with a microphone, whereby on the anechoic chamber side the

sound intensity is measured with an intensity probe. A comparison is made with a prediction based on the literature. Values regarding the characterization of the chamber were found to be quite coincident with the literature, however sound transmission loss measurements showed some discrepancies compared to the theoretical transmission loss prediction [21].
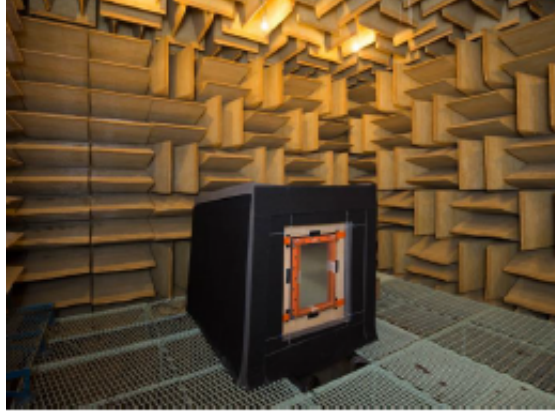
Figure 2.5: Mobile reverberation cabin [21].

Other experiment [22] was carried out to validate the design and construction of a smaller reverberation chamber, where diffusers were placed to better uniform the sound field. Here, is was shown that the construction of a small reverberation chamber with semi-spherical diffusers had impressive diffusion effects. The analysis of the sample (a magnesium alloy plate) was also carried out using the method of the reverberation chamber inserted in a hemi-anechoic as previously stated, although the measurement of sound transmission loss was defined as the difference value of sound pressure level between the two sides. The numerical analysis was carried out using the hybrid method FE-SEA. Results of sound transmission loss results were practically equal to those of the experimental test and so the authors ensured that this model can be useful in future work of acoustic analysis, as illustrated in Figure 2.6.
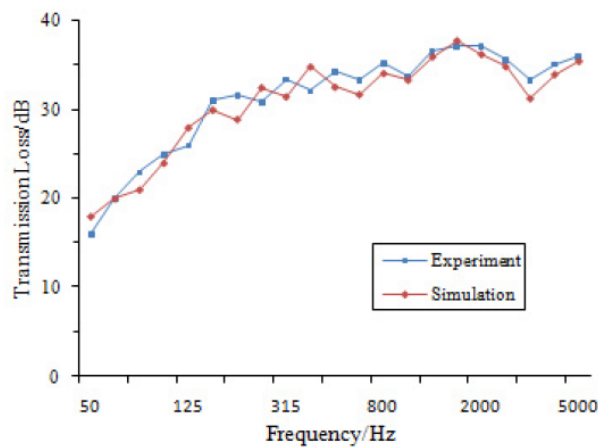
Figure 2.6: FE-SEA: Transmission loss simulation and experiment comparison [22].

2.2   Scan & Paint

Scan & Paint is a method for visualizing time-stationary sound fields, producing high resolution mapping of particle velocity, sound pressure and sound intensity. It has become very useful for sound transmission loss measurements using sound intensity, as well as to detect noise sources or leaks depending on the material or equipment to be analysed.

2.2.1   Procedure

For the scanning of a series of points, study and graphic visualisation of sound fields, the Scan & Paint technique essentially consists of a transducer travelling along a measuring plane, while this whole event is filmed by a camera.

In the post-processing stage, automatic colour detection is applied in each video frame. A spatial discretisation method is then used to divide the collected signals into various segments, assigning a spatial position based on the tracking data. As a result, each signal fragment will be connected to a unique spot on the measurement plane and the analysis of the signal segments is then used to determine spectral variances across the space. At last, results are integrated with a background image of the environment being measured to produce a visual representation that enables the visualization of the sound field [23].

Figure 2.7 explains the process for Scan & Paint measurements.
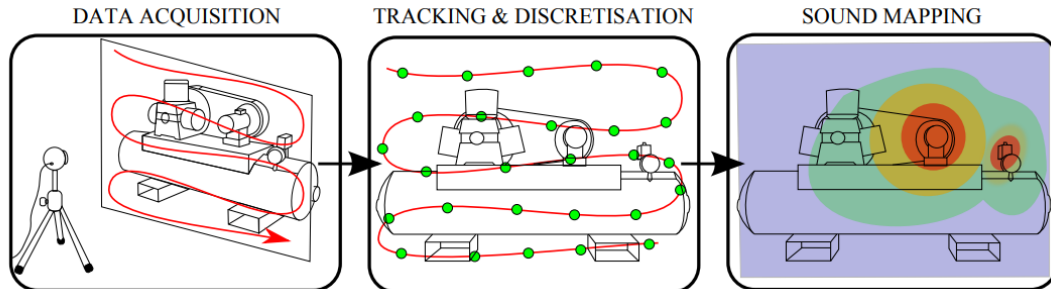
Figure 2.7: Steps for the Scan & Paint measurements [23].

The high flexibility, high resolution and low cost characteristics of the proposed measurement methodology define Scan & Paint as an efficient sound visualization technique, especially for stationary sound fields. It can be useful in vibroacoustic analysis, material characterisation and, more specifically, in obtaining sound transmission loss values [24]. Thus, the experimental procedure is based only on the use of a camera, an intensity probe and a computer equipped with a software dedicated to Scan & Paint.

If a single probe is capable of incorporating particle pressure and velocity, it is possible to carry out a complete study of the sound field, which consequently also makes it possible to ascertain some properties such as impedance, reflection and absorption.

This technique is also used to detect the origin of sound sources in one or more points and, therefore, to detect defects in components or materials [25].

The two most commonly used pieces of equipment for measuring sound intensity are the p-u or p-p type probes. The p-u type probes directly measure the sound pressure and

velocity of the particles, while the p-p type probes are able to measure an approximation of the velocity by determining the pressure gradient with two microphones. Both instruments measure sound intensity according to the mathematical expression defined by

$$I = pv, \tag{2.5}$$

where p represents sound pressure, in Pa, and v represents particle velocity, in m/s.
P-u probes are know to be much more efficient than p-p probes, due to effective measurements in medium and low frequency ranges and even because of the probe geometry itself, which allows systematic errors to be minimised [26].

2.2.2   Tests performed with Scan & Paint

Scan & Paint technology has been used for acoustic treatment and characterization of several devices such as car engines and turbo compressors. A study on an engine cover comparing far field and near field conditions showed good agreement [27]. In another study carried out with focus on stationary sound fields, the authors obtained values for sound pressure and particle velocity by manually moving a p-u probe across a car engine using two different Scan & Paint scanning techniques: point method and grid method [28].
Figure 2.8 shows a measurement performed using the grid method.

Figure 2.8: Measurement tracking (left) and data points of the grid method (right) [28].

The point method deals with a finite number of localized positions, defining a series of spatial positions associated to the audio signal acquired. On the grid method, once the spatial domain of interest has been discretized, it is possible to establish a link between measurement data acquired with a moving transducer and the grid. It is possible to fragment the continuous route into several segments.
The point method has a higher spatial resolution and variance error, but on the other hand the grid method leads to smoother results, converging to an optimal answer when performing longer scans and sweeping several times over the same area. Despite the differences, there is an overall strong agreement between the two methods (Figure 2.9).
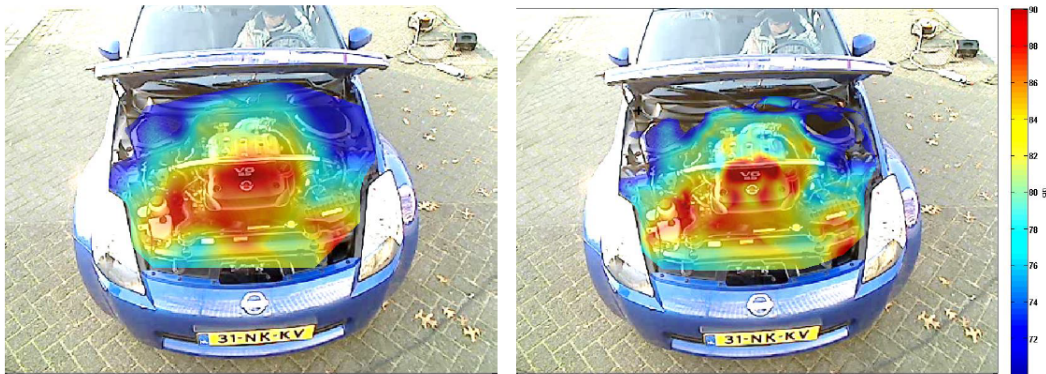
Figure 2.9: Particle velocity mapping with grid method (left) and point method (right) at 150 Hz [28].

Lastly, it was also conducted an experiment using Scan & Paint on a turbo compressor to solve a noise issue in operating conditions (Figure 2.10). The target was for an estimation for sound power, and the authors conducting the tests proved the quickness and reliability of the method [29].
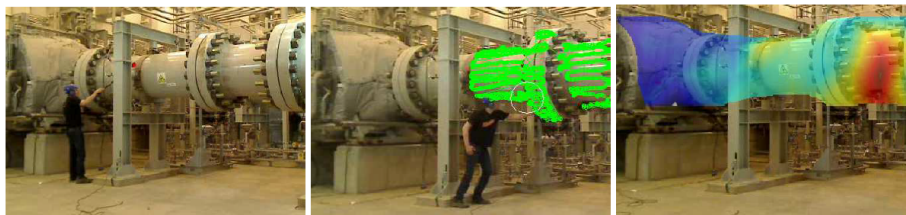
Figure 2.10: Probe tracking and sound mapping on a turbo compressor [29].

2.3 Sustainable materials for acoustic treatment

As a result of growing environmental concern and to reduce the carbon footprint in the production and processing phase of materials, sustainable compounds that preserve their properties when subjected to conditions of use are sought in this field.

2.3.1 Foams

Generally speaking, porous materials like foams have the advantage of relative simple processing, low cost and wide sound absorption range. However, poorer acoustic performance can be noted at lower frequencies due to a strong impedance mismatch.
PUR foams, for example, are widely used in the acoustic field research and industrial applications for soundproofing. PUR foam waste is one of the residues of the manufacturing processes in the textile industry. Therefore, recycling this material to use it for sound insulation purposes is a viable alternative to conventional materials for practical applications. Studies using various numerical models proved that PUR foams present good sound absorbing properties [30]. Figure 2.11 shows an electron microscopy image of a recycled PUR foam.
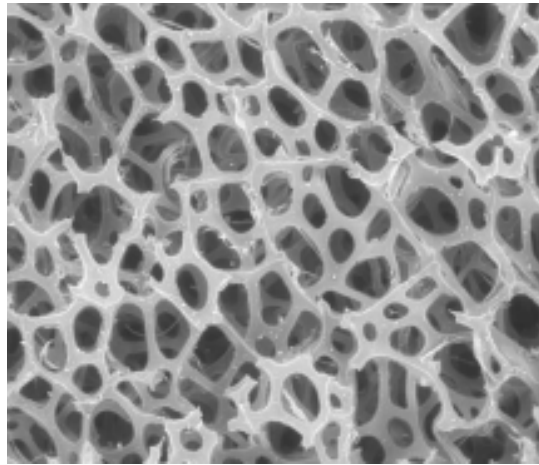
Figure 2.11: Microscopy image of a recycled PUR foam [30].

Sound insulation capabilities are strongly related to pore morphology as high sound absorption efficiency is achieved when smaller pore sizes and more pore numbers are obtained. When treated with external materials such RWF, PUR foams show interesting sound absorption results, with notable improvements in the low frequency range and specially from 400 Hz onwards (Figure 2.12) [31].
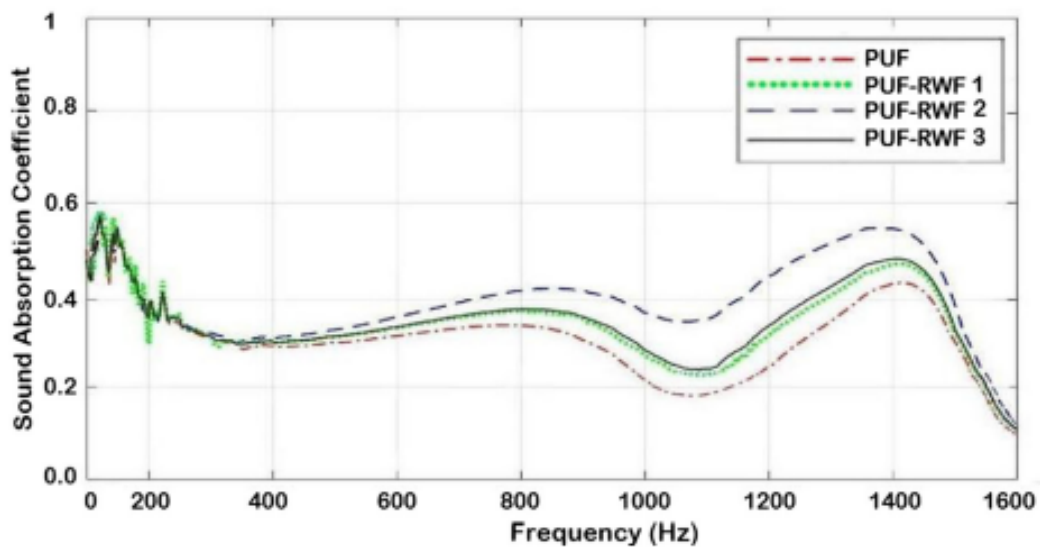
Figure 2.12: Sound absorption coefficient of PUR and PUR with RWF of different contents [31].

Thermoplastic foams are also used for for acoustic treatment and have the benefit of ease in recycling and improved mechanical properties when compared to PUR foams and other textile based sound absorbing materials . Others such as metallic or graphene are used for sound insulation as well, and even though in their case the sustainability aspect may be called into question, these materials have a significant potential to become sustainably produced in the near future [32].

2.3.2   Geopolymers

Geopolymers are a class of aluminosilicate binders synthesised typically at temperatures below 100 °C. Even though geopolymers were initially considered for several applications, through the years they have been considered an alternative to ordinary Portland cement, primarily due to their lower embodied CO_2 [33]. These materials and in particular geopolymeric foams are very promising for several engineering applications, as a result of their low cost, sustainable nature and good properties.

Geopolymers have come to excel as materials for acoustic treatment, namely geopolymers based on aluminium waste and geopolymer foams. Acoustic properties are deeply linked to the porous structure of the porous geopolymers since sound absorption is associated with the friction-energy loss in the wall of pores in a porous material. Sound absorption coefficient is also related to the pore size, tortuosity and permeability in the pore network. However, if the open porosities are very high, the impact of sound in the walls of the porous structure is reduced, diminishing its sound absorption [34].

An experiment regarding geopolymers based on aluminum waste indicated that sound absorption was higher in medium frequency ranges (650 Hz – 1600 Hz) and again in high frequency ranges, from 3500 Hz upwards. As open porosity was increased, acoustic properties were significantly improved [35].

On the contrary, GFC indicated very high sound absorption in low frequencies, from 40 Hz to 150 Hz, but decreases dramatically afterwards, just slightly increasing again after 800 Hz (Figure 2.13). It was also proven that in this frequency region, the increase of the samples' thickness improves sound absorption [36].

(a) GFC cross section.   (b) Sound absorption for selected GFC.
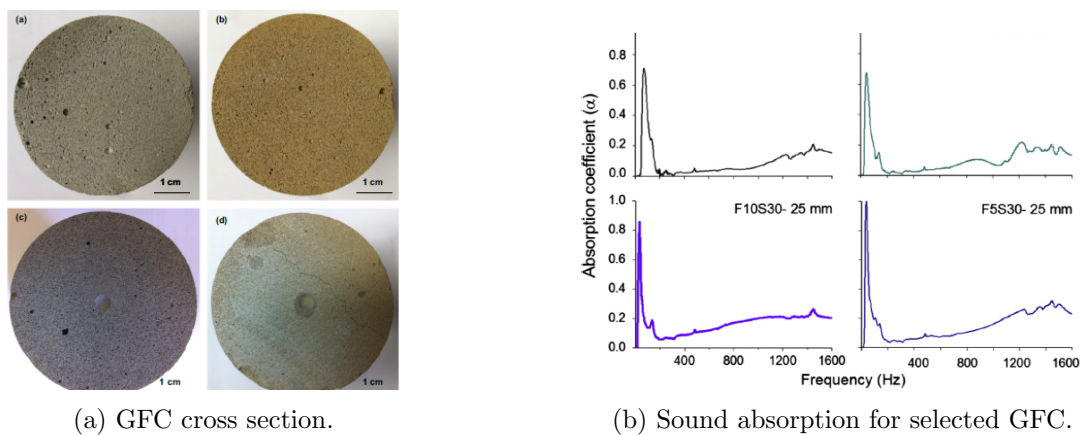
Figure 2.13: Experiment with geopolymer foam concrete [36].

Geopolymeric foams with silica fume as foaming agent reveal an increase in sound transmission loss as the frequency increases as well and generally, if silica fume content increases, so does sound insulation effect. These materials show great potencial for the fabrication of geopolymeric foams due to environmental benefits and lower costs [37].

Regarding sand mixtures, a study was made where two compositions with different quantities of quartz sand have been tested. In each composition, there were also studied two thicknesses for each case (10 mm and 30 mm for the first case; 20 mm and 30 mm for the second case). It was observed that the use of two different fractions of quartz sand

improves maximum absorption coefficients. Overall, results are similar and both cases show that bigger thicknesses result in higher sound absorption coefficient up to around 1600 Hz. However, there is a turning point in the specific frequency as reduced thickness shows higher sound absorption coefficients from there [38].

An experiment with lightweight composites produced from geopolymer paste with the incorporation of different organic type wastes including expanded polystyrene and tire rubber was also conducted. Here, it was observed a maximum absorption coefficient of 0.7 at 500 Hz of polystyrene composites and 0.6 at 700 Hz for rubber composites [39].

2.3.3 Cork

Cork is a material that combines low density and high porosity, provides excellent acoustic insulation and is sustainable. The implementation of cork in some agglomerates proves to be very effective, since the use of this material from the order of 75% vol. shows high sound absorption coefficients. Generally, it was verified that when the amount of cork in the agglomerate is increased, the levels of sound absorption increase in high frequency ranges and so does the overall acoustic performance of the composite [13].

The use of cork containing recycled inorganic polymeric composites also shows good sound absorption coefficients from 1000 Hz frequency onwards, showing a substantial growth until around 2000 Hz, with a decrease at higher frequencies (Figure 2.14). Not only is the volume of cork responsible for the sound absorption patterns in composites of this kind, but also the size of the cork granulate itself [40].

(a) Inorganic polymers with cork.   (b) Sound absorption of inorganic polymer with cork.
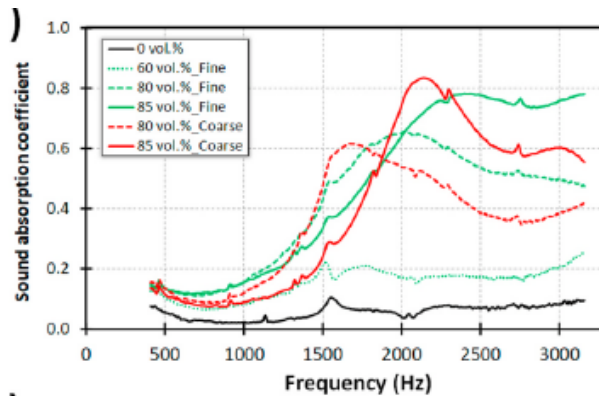
Figure 2.14: Study with cork containing waste derived inorganic polymer composites [40].

2.3.4 Wood

Wood has been a material of choice for acoustic performance for centuries. It is used in musical instruments and other applications that include architecture and engineering, serving as a material for acoustic treatments and sound deflection [41]. Wood may not be dense enough to absorb much sound. However, enhancing wood's porous nature can improve its sound absorption ability, since wood with holes cut into it becomes a perforated resonator that does reduce sound [42].

A work to evaluate the sound insulation provided by woods of different densities concluded that there was a drop in sound insulation when using woods with lower bulk density [43].

Wood plastic composites have found a wide applicability in many industrial as a result of economic competitiveness and good mechanical and acoustic properties in comparison to traditional materials.

It was conducted a numerical and experimental vibroacoustic analysis of a panel made out of WPC boards of high density polyethylene filled with 50 wt% of wood fibers from pine sawdust (Figure 2.15). The WPC sample was mounted into the testing window between a reverberation chamber and a hemi-anechoic chamber. Speakers were placed in the reverberation chamber, emitting stationary white noise and the average sound pressure level was measured using six microphones. From the hemi-anechoic chamber, sound intensity was measured by a manual scanning procedure using a sound intensity probe.

Sound transmission loss was obtained according to the ISO 15186-1 standard. There was good approximation between the finite element simulations and the sound transmission loss measured in the laboratory. Results revealed that in the low frequency range there is reduced sound transmission loss (15 dB to 26 dB), with a slight increase in the next frequency intervals. At high frequencies, close to 5000 Hz, sound transmission loss peaked at near 45 dB [44].

Figure 2.15: WPC view from the reverberation (left) and hemi-anechoic chamber (right) [44].

Chapter 3

Theoretical Background

A theoretical background on some essential acoustic principles is presented in this chapter for a better understanding of the work.

3.1 Acoustic principles

Sound can be defined as a wave motion in air, other elastic media such as liquids or solids or as that excitation of the hearing mechanism that results in the perception of sensation. Without a medium, sound cannot be propagated.

3.1.1 Sound waves

Sound propagates in the form of longitudinal waves, involving successive compressions and rarefactions in the elastic medium (Figure 3.1). When a vibration occurs, the sound wave advances evenly. Each molecule will move a specific amount to the right and subsequently a similar amount to the left of its undisplaced position, causing pressure changes, ultimately characterizing sound behaviour [45].

C = Compression (region of high pressure)
R = Rarefaction   (region of low pressure)

Direction of sound wave
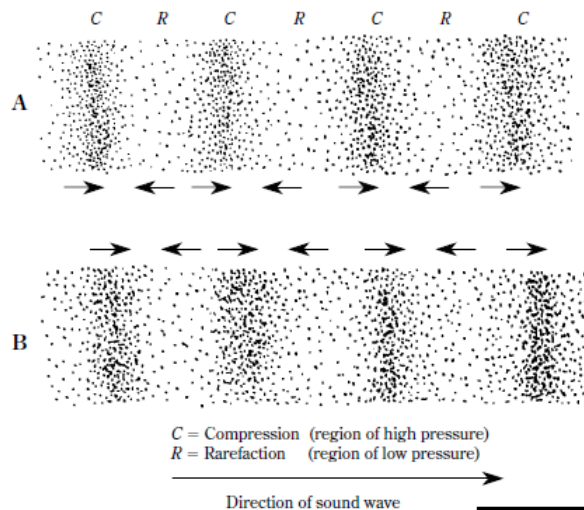
Figure 3.1: Propagation of sound [45].

The wave equation for a three dimensional system is described by

$$\nabla^2 p - \frac{1}{c^2}\frac{\partial^2 p}{\partial t^2} = 0, \tag{3.1}$$

in which p is the pressure and c is the speed of sound [46]. There are four major variables that characterize sound waves [47]:

- **Frequency** (f) - Number of pressure variation cycles in the medium per time unit. It is expressed in Hertz (Hz), in memory of german physicist Heinrich Hertz.

- **Wavelength** (λ) - Distance a wave travels in the time it takes to complete one cycle. A wavelength can be measured either between successive peaks or between any two corresponding points on the cycle.

- **Period** (T) - The time taken for one cycle of a wave to pass a fixed point. It is measured in second (s) according to the international system of units (SI) and relates to frequency by

$$T = \frac{1}{f} \tag{3.2}$$

- **Pressure changes** - Maximum pressure amplitude, p_M, or the root-mean-square (RMS) amplitude, p_{rms}. It is expressed in Pascal (Pa). Root-mean-square means that the instantaneous sound pressures are squared, averaged and the square root of the average is taken.

The general equation for wave propagation would be

$$\phi = g(c_0 t - x) + h(c_0 t + x), \tag{3.3}$$

with g and h being arbitrary variables, x is the direction in which the wave travels and c_0 the velocity. As for particle velocity in regard to particle pressure, it can be obtained as [48]

$$u = -\frac{1}{\rho_0}\int(\frac{\partial p}{\partial x} + \frac{\partial p}{\partial y} + \frac{\partial p}{\partial z})dt. \tag{3.4}$$

3.1.2   Conversion to the decibel scale

Perception of sound is not linearly related to the quantities used to characterize sound waves and so, a logarithmic scale called level scale was developed. The decibel (dB) is created by adding a factor of 10 to prevent creating a scale that is too compressed for the human ear sensitive range. Ear is more sensitive to intensity ratios than intensity differences. A quantity level is determined as the base 10 logarithm of the ratio of a quantity, such as energy, to a reference value for that quantity. In acoustics, the decibel is used to quantify sound pressure levels that people hear, sound power levels radiated by sound sources or the sound transmission loss through a surface.

3.1.3   Sound pressure

Sound pressure is a scalar quantity that indicates the level of sound amplitude at a certain location in space. The volume changes depending on where and how far away from the sound source the sound is heard. Sound pressure is measured in Pascal (Pa) and sound pressure level, measured in dB, is defined by

$$SPL = 10 \log_{10} \frac{p_{RMS}^2}{p_{ref}^2} \quad \text{(dB)}. \tag{3.5}$$

In this case,

$$p_{RMS} = \frac{p_{max}}{\sqrt{2}} \ , \tag{3.6}$$

where p_{max} is the amplitude of the acoustic pressure wave and $p_{ref} = 20\mu$Pa RMS. This reference pressure corresponds to the smallest sound that a young, healthy human ear can pick up when it happens in the range of frequencies where hearing sensitivity is greatest, around 1000 Hz [49].

3.1.4   Sound intensity and sound power

Sound intensity is vectorial, with both a direction and a magnitude and product of sound pressure and particle velocity in the direction of the intensity vector. It is a measure of the rate at which work is done on a conducting medium by an advancing sound wave and thus the rate of power transmission through a surface normal to the intensity vector. Being the amount of sound energy radiated through an unit area, it is expressed in Watt per square meter (W/m^2).
The intensity in the direction of propagation of a plane or spherical free-progressive sound wave, in the absence of reflected sound waves and far away from the source, is given by

$$I = \frac{p_{RMS}^2}{\rho_0 c} \quad \text{(W/m}^2\text{)} \tag{3.7}$$

where ρ_0 represents the fluid's density (kg/m^3) and c the speed of sound (m/s).
Converted to the decibel scale, sound intensity level (L_I) can be defined by

$$L_I = 10 \log_{10} \frac{I}{I_{ref}} \quad \text{(dB)} \tag{3.8}$$

and I_{ref}=10^{-12} W/m^2.
The total sound energy radiated by a sound source per unit time is the sound power, measured in Watt (W). It is defined as the rate at which sound is emitted from an object, regardless of the location or distance from which the sound is observed. Sound power measurements are often specified in the noise regulations of many different kinds of products, from construction equipment to computer printers. It is closely related to sound intensity, as it is obtained by integrating the sound intensity over the cross area where the sound wave travels through. So it is expressed by the following equation:

$$W = \int \vec{I} \cdot d\vec{s} \tag{3.9}$$

Similar to sound intensity, in the decibel scale, sound power level (L_w) is defined by

$$L_w = 10 \log_{10} \frac{W}{W_{ref}} \quad \text{(dB)} \tag{3.10}$$

and $W_{ref}=10^{-12}$ W. These two quantities can be related in different ways, depending on the nature of the sound wave, as shown in Table 3.1. Q represents the directivity factor, which is dimensionless and is connected to the frequency and direction of the sound wave, and r is the distance to the sound source.

Table 3.1: Relation between the sound intensity and the sound power per unit area (S).

Plane waves	I=W/S
Spherical	I=W/$(4\pi r^2)$
General	I=QW/$(4\pi r^2)$

3.1.5   Octave bands

Mechanical devices such as engines, fans and compressors typically generate and radiate noise throughout the audible range of the human ear.

Humans are more sensitive to frequency ratios than frequency differences, hence frequency ranges often contain lower and upper frequencies that are related by the same ratio.

Octave bands provide a filtering method for dividing the audible spectrum into smaller segments called octaves. This can be used to identify different noise levels at individual frequencies. Each octave band can be further divided into providing the 1/3 octave bands.

One third octave bands are mainly used in environmental and noise control applications. Laboratory data for sound pressure, sound power and sound intensity levels, as well as sound transmission loss, can be expressed as 1/3 octave band levels.

A "one-third octave" can be defined as one third of an octave, corresponding to a frequency ratio of $2^{1/3}$, according to the ISO 18405:2022 [50]. The spectrum from 20 Hz to 20 kHz can be divided into thirty one 1/3 octave bands.

In a general manner, the middle frequencies of an n-th octave bands are obtained by successive multiplication or division of 1000 Hz, which is the reference middle frequency in acoustics, with $2^{1/n}$. The lower and upper frequency bounds of a given n-th octave band with middle frequency f_0 are given by $f_0/(2^{1/2})^{1/n}$ and $f_0(2^{1/2})^{1/n}$ respectively.

Table 3.2: Octave bands frequencies.

	Octave	**1/3 Octave**
Middle frequency	f_0	f_0
Lower frequency bound	$f_0/2^{1/2}$	$f_0/2^{1/6}$
Upper frequency bound	f_0 x $2^{1/2}$	f_0 x $2^{1/6}$

3.2   Conditions for sound transmission loss measurements

When a sound wave impacts against an acoustic barrier, part of its energy is reflected, absorbed or transmitted. Thus, there will be a sound transmission loss to a degree dependent on the characteristics of the sound barrier. The greater the sound transmission loss, the greater the sound attenuation capacity of a certain surface, such as a door, a wall or an insulation material.

Sound transmission can be classified into two main types: direct and marginal. Direct transmission is characterised by the propagation of sound waves directly through the separation element, whereas marginal transmission refers to transmission via adjacent paths other than the separation element. Transmission loss in acoustics is the reduction in sound intensity brought on by a barrier or other structure at a specific frequency. As stated previously, sound transmission loss measurements can be divided in two ways: sound pressure or sound pressure-intensity measurements.

3.2.1   Free field

Anechoic chambers are enclosures with sound absorption of 99% or more, or less than 10% reflection. Not only are anechoic chambers intended to be echo-free spaces, but they are also intended to be sound-proof spaces. In laboratory, these rooms are used to simulate a free field condition (Figure 3.2).
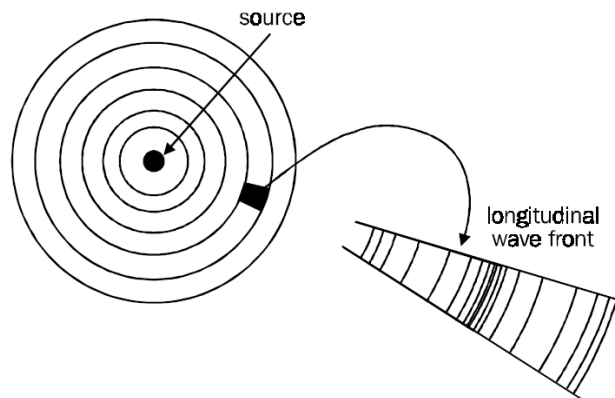
Figure 3.2: Radiation of sound from a simple source in a free field [47].

This technically means that sound pressure level from a radiating sound source in the chamber should decline by 6 dB for every doubling of distance from the source. Sound should be able to travel in straight lines, unimpeded and undeflected. Also, there should not be any interference from outside noise or extreme changes in humidity, pressure, or temperature [48]. The common sound absorbing materials for building these chambers include porous materials, such as wedge-shaped, perforated sheet metal wedges or specific acoustic foam, filled with fiberglass insulation or acoustic tiles. As for hemi-anechoic chambers, they are slightly different as the floor is a normal reflecting plane. Anechoic and hemi-anechoic chambers are typically used for sound transmission loss measurements using sound pressure level and sound intensity.

In an anechoic chamber or free field, it is often desirable to mathematically describe the acoustic radiation of a omnidirectional source [51]. In this case, the sound wave spreads out as it moves away from the source, and the wavefront is always spherical. The wave equation in spherical coordinates is

$$\frac{\partial^2 p}{\partial r^2} + \frac{2}{r}\frac{\partial p}{\partial r} = \frac{1}{c^2}\frac{\partial^2 p}{\partial t^2}, \tag{3.11}$$

where r represents the distance from the origin of the coordinate system or source and this equation assumes equal radiation in all directions.

3.2.2   Diffuse field

On the other hand, reverberation chambers are used in measurements to simulate a diffuse sound field. In a diffuse sound field, sound waves arrive simultaneously from all directions with equal probability and level. Basically, sound pressure is the same at any point in the chamber. According to the Sabine-Franklin-Jaeger theory, sound fills a reverberant room in such a way that the average energy per unit volume in any region is nearly the same as in any other region [46]. To achieve a diffuse sound field, reverberation chambers are designed in a very unique way following a few principles [48]. Some of those are highlighted next:

- **Reflecting surfaces** - Hanging objects from the ceiling gives the spaces highly reflecting surfaces. For a given room volume, this enhances the sound reflecting area without significantly increasing the room absorption. Many reflections hence improve the sound dispersal.

- **Non-parallel walls** - With such a setup, the sound waves in the space can randomly impinge at different incidence angles on the walls. The total number of normal modes for an irregularly shaped room is almost equal to that for a room with parallel walls when the volume remains constant. Yet, in a room with an irregular form, the degeneracy of modes caused by the overlap of modal patterns is far lower, and as a result, a more diffuse sound field is created.

- **Multiple frequency sound source** - Signals such as warble tones (frequency-modulated tones) and 1/3-octave noise have energy over a wider range of frequencies than pure tones. Such a source can generate a series of modal patterns, each providing a tightly grouped frequency band. The application of such sound sources is usually necessary and independent of chamber design and construction.

Reverberation time is the time required for sound to decay in a closed space after the sound source stops. Factors affecting it include the volume of the room, type of materials and surface area of material. Usually, the exponential decay of reverberant sound is defined by the time (T_{60}) required for the spatial average of the energy density to drop by 60 dB. Sabine's equation for an empty chamber of volume V reveals that

$$T_{60} = \frac{0.161 \cdot V}{\sum_i \alpha_i A_i} \tag{3.12}$$

in which α_i is the sound absorption coefficient of the walls' covering [46].

Reverberation chambers are used in sound transmission loss measurements using sound pressure level. It is of great importance for the construction of the chamber to ensure modal frequencies and equal spacing between modes, as well as the position of the sound source and microphones.

Regarding acoustic tests in reverberation chambers, a sample is placed on the floor and the reverberation time is measured. Then, a comparison is made with the reverberation time with the chamber empty, obtaining the number of absorption units that the sample adds to the chamber and, consequently, the absorption assigned to each unit of area of the sample is determined, giving the equivalent absorption coefficient. Regarding the two reverberation chamber method using sound pressure, the Equation 2.1 defines the value for sound transmission loss.

3.2.3   Sound transmission through a panel

Considering a chamber in which reverberant energy density is $\overline{w}_{in}$, the energy incident per unit time on a panel of area ΔA is $(c/4)\overline{w}_{in}\Delta A$ [46]. Some of the energy is reflected, a fraction is dissipated within the panel and a fraction is transmitted (Figure 3.3).
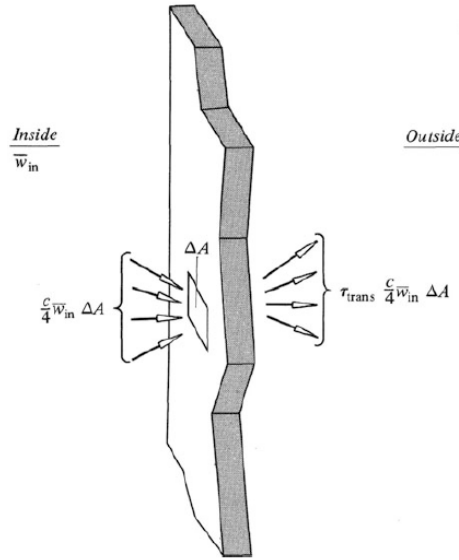
Figure 3.3: Reverberant sound transmission through a panel [46].

Generally, transmission loss of a segment under consideration is defined as

$$R_{TL} = 10 \log \frac{1}{\tau_{trans}} \tag{3.13}$$

and the ratio of total energy transmitted to total energy incident is

$$\tau_{trans,ri} = 2 \int_0^{\frac{\pi}{2}} \tau_{trans}(\theta) \cdot sin\theta \cdot cos\theta d\theta. \tag{3.14}$$

The corresponding ratio of local volume averages of mean squared pressures is

$$\frac{\overline{p_{out}^2}}{\overline{p_{in}^2}} = \frac{1}{2} K \cdot \tau_{trans,ri} \tag{3.15}$$

$$K = \frac{\int_0^{\frac{\pi}{2}} \tau_{trans}(\theta) sin\theta d\theta}{2\int_0^{\frac{\pi}{2}} \tau_{trans}(\theta) sin\theta cos\theta d\theta}. \tag{3.16}$$

Taking K = 1, when τ is independent of θ:

$$\overline{L_{out}} = \overline{L_{in}} - R_{TL} - 3 \quad \text{(dB)} \tag{3.17}$$

Here, L_{out} and L_{in} represent sound pressure levels [46]. This expression may be subject to some variations according to the procedure, as shown previously.

3.2.4   Acoustic transducers

Microphones

A microphone converts sound energy into electrical energy or, more simply put, sound waves into audio signals.
A diaphragm made of thin material like plastic resonates in response to incoming sound waves and a coil attached to the diaphragm moves back and forth along a permanent magnet. This creates a magnetic field and the current flows out of the coil as a microphone signal output. Figure 3.4 shows a schematic representation of the microphone working principle.
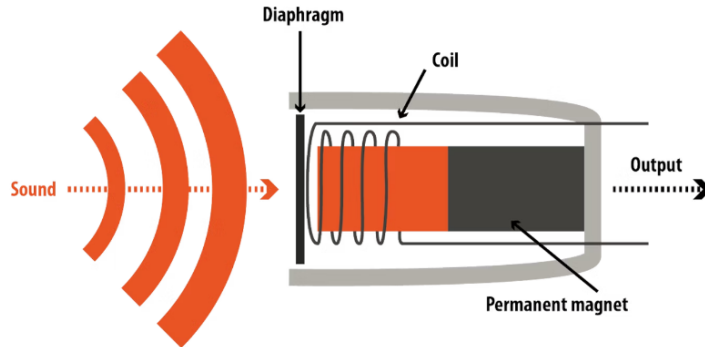
Figure 3.4: Microphone working principle [52].

In the context of this work, free field microphones are quite important. As the name suggests, these are meant to be used in free field environments, such as anechoic or hemi-anechoic chambers. They are mainly designed to capture the sound pressure level from a single source and are pointed directly at the sound source [52]. Thus, free field microphones are usually used in loudspeaker and appliance testing, such as washing machines, blenders or heat pumps. Figure 3.5 shows an example of a free field microphone.

Figure 3.5: Free field microphone [52].

Sound intensity probes

Intensity probes are useful in sound intensity Scan & Paint measurements, which are based on the acquisition of particle velocity and sound pressure.

Particle velocity is the local speed of a fluid travelling backwards and forwards due to a moving surface which displaces a volume. As a result, this magnitude is proportional to the displacement of the excitation source. The value of this quantity might be either positive or negative depending on the flow direction. The magnitude of particle velocity can be given by

$$\vec{u}(t) = \frac{\partial \xi}{\partial t} \tag{3.18}$$

where ξ represents particle displacement. Considering only normal velocity, this equation can be related to the pressure by

$$u_n(t) = -(\frac{1}{\rho_0}) \int_{-\infty}^{t} (\partial p(\tau)/\partial \vec{n}) d\tau \tag{3.19}$$

where ρ_0 represents the density of air and p the sound pressure [26].

The p-u probes for Scan & Paint measurements involve the combination of a pressure microphone with a particle velocity transducer. It is the only way to measure acoustic particle velocity directly. Figure 3.6 shows an example of a sound intensity probe. In the image, particle velocity sensor can be seen on the solid cylinder (right) and the electret microphone is mounted inside the other cylinder (left).
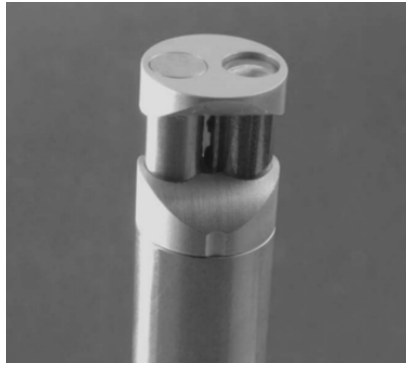
Figure 3.6: Sound intensity probe [53].

Sound intensity is the time average of the instantaneous product of the pressure and particle velocity signal,

$$I_r = (pu_r)_t = \frac{1}{2}\text{Re}\{pu_r^*\}. \tag{3.20}$$

However, the pressure and the particle velocity transducer will have different phase responses, which may lead to serious consequences under certain conditions.

As for p-p probes, an estimation for sound intensity is made using an approximation method. Particle velocity in the direction of the axis of the probe is obtained by a finite-difference approximation to the pressure gradient between two pressure microphones near each other [53]. An approximation of the sound intensity can be made using the following equation [26]:

$$I_n(t) \approx (1/2\rho_0 d)[p_1(t) + p_2(t)] \int_{-\infty}^{t} [p_1(\tau) - p_2(\tau)] d\tau. \tag{3.21}$$

After the manual or automated measurements with the probe, in the post-processing stage of the Scan & Paint technique there is an automatic colour detection to each frame of the video, as previously stated. It is then possible to split the long recording into multiple segments by applying a spatial discretization via a point method or a grid algorithm [28].

It is possible to define a sequence of spatial positions associated with the collected audio signal since there are finite number of localized positions, such as

$$\vec{\Gamma}_i = (x_1, y_i) \quad / \quad \vec{\Gamma}_i \in \Omega_h \tag{3.22}$$

with $i \in \mathbb{N}$ indicating the position index. Each of the tracking samples is associated with a time interval. The discretization process is made along the scanning route $\vec{r}(t)$ depending on the following parameters: number of averages (n_d), sample block width (B) and overlap between sample blocks (o_d). Each time interval is defined as

$$\tau_i = [\frac{i}{f_v} - \frac{n_d B o_d + o_d}{2f_s}, \frac{i}{f_v} + \frac{n_d B o_d + o_d}{2f_s}], \tag{3.23}$$

where f_v and f_s denote the video and audio sampling frequencies, respectively. The whole length audio signal in the given time frame is then evaluated to determine the pressure and particle velocity levels appropriate for each spatial position,

$$\mathbb{P}(\vec{\Gamma}_i) = p(\tau_i) \tag{3.24}$$

$$\mathbb{U}(\vec{\Gamma}_i) = u_n(\tau_i). \tag{3.25}$$

Chapter 4

Improvements of test conditions

The developed reverberation chamber used as the testing system is unable to incorporate samples with different thicknesses, being limited to samples with 40 mm of thickness. Thus, it was necessary to develop a mechanism able to adjust the thickness of the compartment so that samples with different thicknesses can be tested and that, therefore, could also save some work in terms of pre-test sample treatment, regarding sample cutting, for example. The target for the maximum sample thickness was considered to be 45 mm.

Also, in order to perform the tests with a higher degree of accuracy, an automated XY system based on a 3D printer working principle was used. Even though it is possible to manually scan the sample plane, a few errors can occur mainly connected with imprecisions with the measurements and inaccurate distances between the intensity probe and the sample plane.

Figure 4.1 shows the chamber and test setup before the improvements.

(a) Initial chamber condition.   (b) Manual scan.

Figure 4.1: Test setup before improvements.

4.1 Sample holder

The sample holder is the compartment where the samples are put in order to be tested. It consists of two components:

- A plate with a hole with the dimensions of the sample, where the sample will be put, in contact with the chamber - "mother plate".

- A plate to hold the sample and to prevent it to fall or move during the tests - "cover plate".

The mother plate had initially 27 mm of thickness , while the cover plate was 13 mm thick. Aiming to test a maximum of 45 mm thick samples, a new mother plate was designed for the compartment to allocate 40 mm samples and for its production to be simpler. As for the cover plate, it was designed with a 5 mm wide compartment for the allocation of the samples, in case of samples with a thickness between 40 and 45 mm.

Sample slips or sound leaks might occur during testing, so it is imperative for the samples to remain compact and well connected to the sample holder supports, ensuring uniformity of tests and to prevent the adulteration of the results regarding sound transmission loss measurements. More importantly, in the case of tests with samples with small thickness there is a need for some type of support to prevent samples from falling, slipping away and make sure they are rigid and in contact with the mother plate without any leaks. For this effect, a frame was designed to compact the samples. Its positioning, depending on the thickness of the sample, can be adjusted with screws. Therefore, it is possible to test samples of different thicknesses, guaranteeing the repeatability and homogeneity of the tests, as well as greater security in terms of certifying that the results are reliable.

Figure 4.2 represents the concept for the frame. It was designed with a 5 mm edge to prevent the possibility of it falling while assembling the components. To interfere as little as possible with the sound transmission results due to its properties, the aluminium frame was designed with a large central cut out, as well as to facilitate the visualization of the samples' sound map during the Scan & Paint analysis.

Figure 4.2: Frame

Figure 4.3 shows the cover and mother plates.

(a) Cover Plate.   (b) Mother Plate.
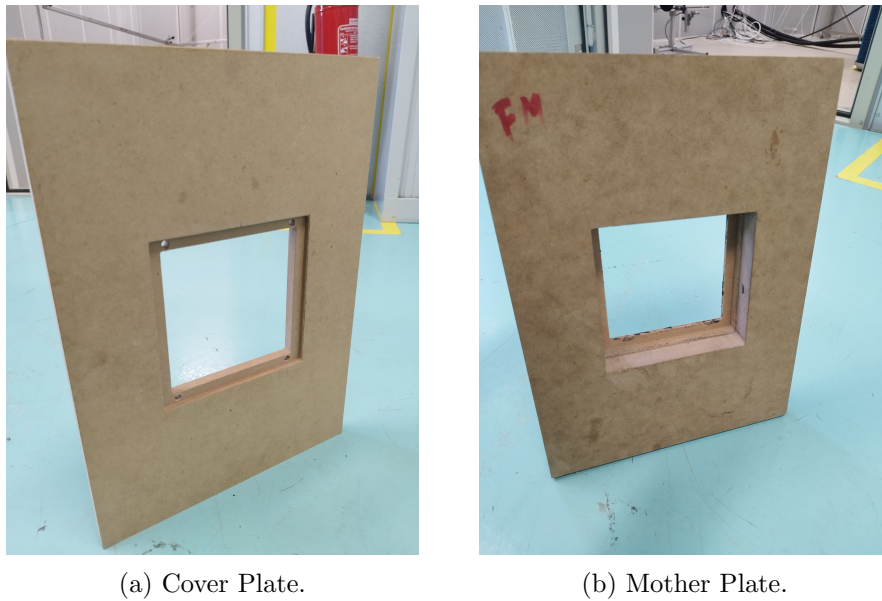
Figure 4.3: Sample Holder plates.

The cover plate was designed with four holes for the fixation of M6 screws to tighten the frame to the sample. Depending on the desired sample thickness for the sound transmission loss analysis, it is possible to adjust the screws in order to tighten or loosen sample in contact with the frame.

Figure 4.4 shows the procedure on how to assemble all the components for sample testing. As previously stated, the maximum sample thickness is 45 mm, but they can be as low as 5 mm. The sample holder placed in the chamber is presented in Figure 4.5.

(a) CAD concept.   (b) Sample Holder.
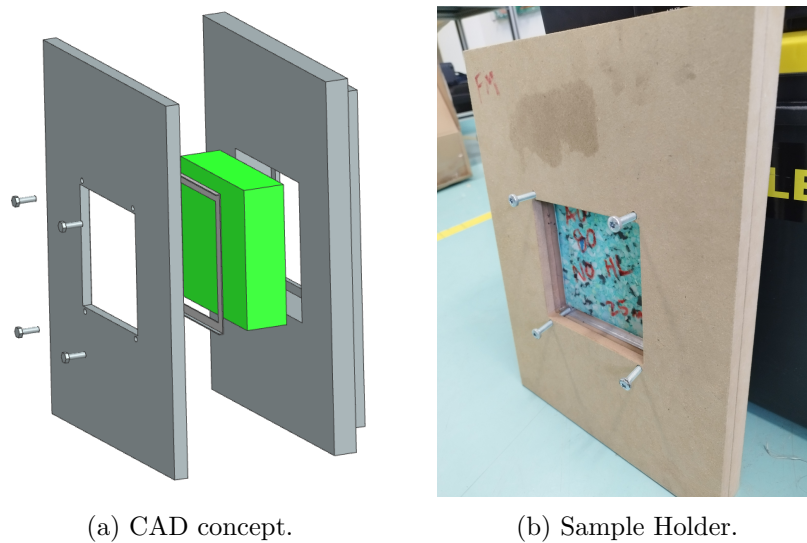
Figure 4.4: Sample holder assembly.

Figure 4.5: Sample holder in the reverberation chamber.

4.2   Scan & Paint Automated System

In order to achieve more effectiveness and reducing the human error while performing measurements, the testing procedure was improved with the development of an automated scanning system to assure uniform and repeatable sample testing.

The main goals are to maintain constant scanning speed, as well as to keep the same distance between the intensity probe and the sample plane for the entire duration of the scans. Keeping the probe fixed and the sensor facing the sample plane during the measurements is also important, such as ensuring the correct orientation of the probe, parallel to the sample.

Therefore, for this purpose, a 3D printer was used as the basic component to perform the automated scans, as shown in Figure 4.6 [54].

Figure 4.6: Ender 3 - 3D Printer.

4.2.1   Fixation elements

Since there was no need for components such as the base frame, bed and the filament holder, all of those components were first promptly removed. However, components such as the power supply and the cooling fan cause some noise that would unquestionably affect the sound transmission loss values.

In the extruder carriage there was mounted a fixation element to an aluminium bar, as shown in Figure 4.7. Then it was assembled a holder for the intensity probe, in order for it to be kept parallel to the sample to be tested. Figure 4.8 shows the probe holder. At last, Figure 4.9 presents the 3D printer with the mentioned components assembled.

(a) Fixation element.
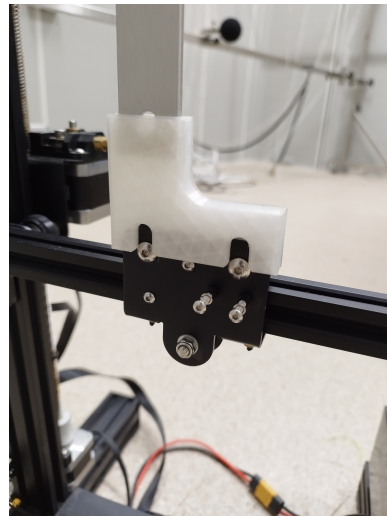
(b) Extruder carriage fixation.

Figure 4.7: Fixation piece on the extruder carriage.

(a) Probe holder.
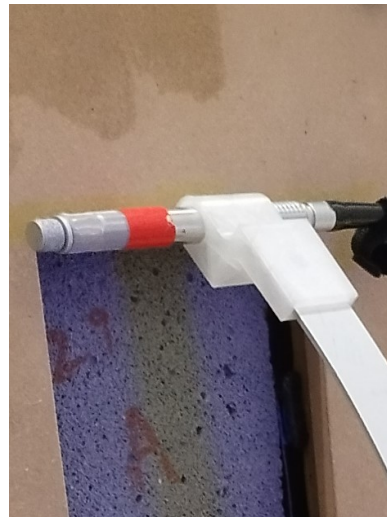
(b) Aluminium profile fixation.

Figure 4.8: Intensity probe holder.

Figure 4.9: Improved scanning system.

4.2.2 Automatic scanning

According to the ISO 15186-1 standard for laboratory measurements of sound insulation using sound intensity, the sample plane must be scanned in parallel lines turning each edge, as Figure 4.10 shows.

Figure 4.10: Scanning pattern for sample plane.

Hence, some G-Code commands were written using the Notepad++ editor in order to test the scanning routine to be transferred to the Ender 3 printing machine. The horizontal lines were written first, followed by the vertical lines, as illustrated in Figure 4.11, although the opposite could be done as well.

```
G28 ; Homing routine
G90 ; Absolute positioning                    ;Start vertical movements
G21 ; Milimeters                              G0 X155 Y0 Z155 F9000
                                              G3 X130 Y0 Z155 R10; First curve vertical
G92 X5 Y0 Z155 ; Set position as original
                                              G0 X130 Y0 Z5
; Start Scanning movement                     G2 X105 Y0 Z5 R10 ; Second curve vertical
; Start horizontal movement
G0 X155 Y0 Z155 F6000 ; set feedrate          G0 X105 Y0 Z155
G2 X155 Y0 Z130 R10 ; First curve horizontal  G3 X80 Y0 Z155 R10; Third curve vertical

G0 X5 Y0 Z130                                 G0 X80 Y0 Z5
G3 X5 Y0 Z105 R10 ; Second curve horizontal   G2 X55 Y0 Z5 R10; Fourth curve vertical

G0 X155 Y0 Z105                               G0 X55 Y0 Z155
G2 X155 Y0 Z80 R10 ; Thrid curve horizontal   G3 X30 Y0 Z155 R10 ;Fifth curve vertical

G0 X5 Y0 Z80                                  G0 X30 Y0 Z5
G3 X5 Y0 Z55 R10 ; Fourth curve horizontal    G2 X5 Y0 Z5 R10; Sixth curve vertical

G0 X155 Y0 Z55                                G0 X5 Y0 Z155
G2 X155 Y0 Z30 R10 ; Fifth curve horizontal
                                              ; Stop programme
G0 X5 Y0 Z30                                  M00
G3 X5 Y0 Z5 R10 ; Sixth curve horizontal

G0 X155 Y0 Z5
```

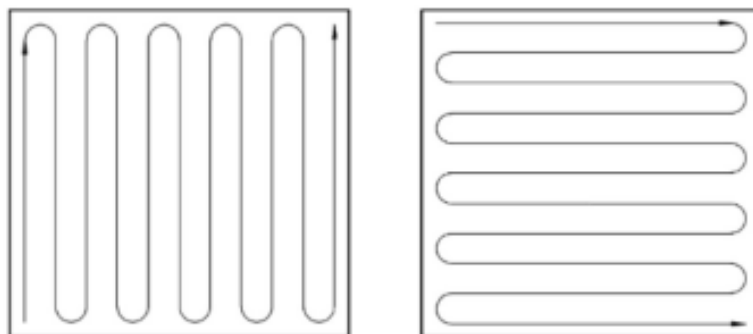(a) G-Code commands for horizontal lines.   (b) G-Code commands for the vertical lines.

Figure 4.11: G-Code commands for the scanning pattern as indicated in ISO 15186-1.

However, it was later found that the stock firmware does not recognise the G2 and G3 arc moves.

An alternative pattern was used only using a simple linear move command, replicating the one suggested in the ISO 15186-1 standard, only replacing the half circles with an angular pattern at the edges of the sample plane.

Figure 4.12 shows the alternative scanning pattern and Figure 4.13 show the updated G-Code commands for the horizontal and vertical lines, respectively.

Ultimately, the scanning speed was programmed on the controller screen of the 3D printer.
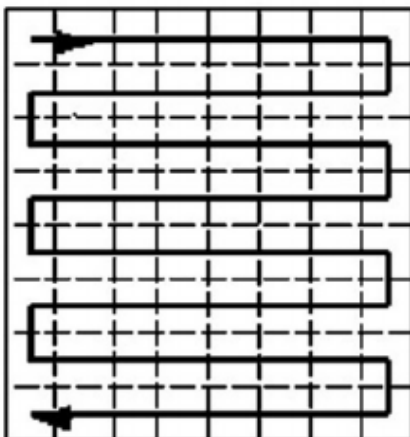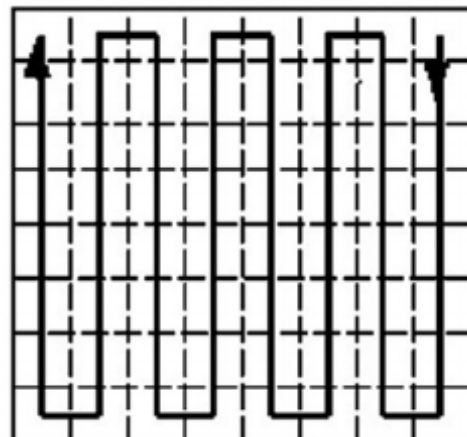
(a) Horizontal movement.   (b) Vertical movement.

Figure 4.12: Alternative scanning pattern used.

```
G28 ; Homing routine
G90 ; Absolute positioning
G21 ; Milimeters ;

; Start Scanning movement
; Start horizontal movement

GO X155 Y0 Z155
GO X5 Y0 Z155

GO X5 Y0 Z140
GO X155 Y0 Z140

GO X155 Y0 Z125
GO X5 Y0 Z125

GO X5 Y0 Z110
GO X155 Y0 Z110

GO X155 Y0 Z95
GO X5 Y0 Z95

GO X5 Y0 Z80
GO X155 Y0 Z80

GO X155 Y0 Z65
GO X5 Y0 Z65

GO X5 Y0 Z50
GO X155 Y0 Z50

GO X155 Y0 Z35
GO X5 Y0 Z35

GO X5 Y0 Z20
GO X155 Y0 Z20

GO X155 Y0 Z5
GO X5 Y0 Z5
```

```
;Start vertical movements

GO X5 Y0 Z155
GO X20 Y0 Z155

GO X20 Y0 Z5
GO X35 Y0 Z5

GO X35 Y0 Z155
GO X50 Y0 Z155

GO X50 Y0 Z5
GO X65 Y0 Z5

GO X65 Y0 Z155
GO X80 Y0 Z155

GO X80 Y0 Z5
GO X95 Y0 Z5 ;

GO X95 Y0 Z155
GO X110 Y0 Z155

GO X110 Y0 Z5
GO X125 Y0 Z5

GO X125 Y0 Z155
GO X140 Y0 Z155

GO X140 Y0 Z5
GO X155 Y0 Z5

GO X155 Y0 Z155

; Stop programme
M00
```

(a) G-Code commands for horizontal lines.

(b) G-Code commands for the vertical lines.

Figure 4.13: G-Code commands for the alternative scanning pattern.

Chapter 5

Materials and Experimental Procedure

Foams and geopolymers are materials of interest for acoustic attenuation in industrial and domestic equipment. This chapter provides a brief description of the materials used for the acoustic tests, as well as how these were conducted. The foam samples tested were supplied by Flexicel, since Bosch also has interest in evaluating the performance of these materials and applying them in heat pumps. The geopolymers were supplied by the University of Aveiro.

5.1 Materials

5.1.1 Foams

Sample materials for testing mainly consisted of several types of bonded foam and a PUR foam. Bonded foam, sometimes referred to as rebonded foam or composite foam, is created utilizing recycled foam from post-consumer and industrial sources. Shredded trim materials are placed in moulds, covered with a binder, and crushed to the necessary density. To create bonded foam blocks, the binder is then activated and cured. They are simple to cut into various shapes for a variety of applications [55]. Tested bonded foams had densities ranging from 60 to 100 kg/m^3 and some of them had bitumen, serving as a heavy layer, providing several testing options (Figure 5.1). The addition of damping layers helps to mitigate the resonant behaviour of materials, improving low frequency transmission loss.

(a) Green bonded foam.   (b) Black bonded foam.   (c) Coloured bonded foam.

Figure 5.1: Different types of tested bonded foams.

As for PUR foams, these are made through basic addition polymerization reaction involving a diol or polyol, a diisocyanate, and water. Sound energy is either propagated by sound pressure waves moving through the fluid within the pores of the polyurethane or due to the elastic stress waves created as a result of the pressure waves, which are carried through the frame of the polyurethane. PUR foams are know to be very effective at attenuating high frequency waves, although exhibiting poor acoustic performance at low frequencies, unless sufficient thickness is used. It has already been proven that an increase in open porosity percentages can generally improve sound absorption through the whole frequency spectrum [56]. The tested PUR foam sample also had a bitumen heavy layer between 13 mm thick specimens of PUR (Figure 5.2).
Table 5.1 indicate tested samples.

Figure 5.2: Bitumen heavy layer within the PUR foam.

Table 5.1: Tested foams.

Type	Density (kg/m^3)	HL	Thickness (mm)	Dimensions (mm)
Black	60	No	25	150 x 150
Black	60	Yes	9 + 2 + 9	150 x 150
Green	100	No	25	150 x 150
Green	100	Yes	9 + 2 + 9	150 x 150
Green	80	No	25	150 x 150
Green	80	Yes	9 + 2 + 9	150 x 150
Coloured	60	Yes	9 + 2 + 9	150 x 150
PUR	222	Yes	13 + 2 + 13	150 x 150

5.1.2   Geopolymers

Porous materials are commonly used in noise control engineering to absorb sound energy. The examined geopolymers (Figure 5.3) are somewhat complex in terms of their components. They are made up of approximately 12% sodium hydroxide and 38% sodium silicate. As for solid components, they contain 15% metakaolin and 35% fly ash, both of which are byproducts of the combustion of biomass in the paper industry. Table 5.2 shows properties and dimensions. A higher percentage of aluminum in the sample translates into an increased porosity, resulting in a density decrease. Moreover, each sample contains 0.05% surfactant, which aids in the development of the structural porosity.

(a) Geopolymers with 0.10% Aluminium.

(b) Geopolymers with 0.15% Aluminium.

Figure 5.3: Tested geopolymers.

Table 5.2: Tested geopolymers with aluminium.

Sample	% Al.	Density (kg/m^3)	Thickness (mm)	Dimensions (mm)
1	0.10	420	20	150 x 150
2	0.10	430	30	150 x 150
3	0.10	470	40	150 x 150
4	0.15	320	20	150 x 150
5	0.15	330	30	150 x 150
6	0.15	390	40	150 x 150

5.2   Test setup

Tests were performed with the small scale reverberation chamber placed inside the hemi-anechoic chamber (Figure 5.4).
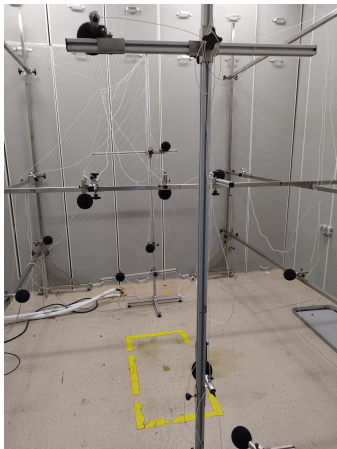
(a) Hemi anechoic chamber.

(b) Reverberation chamber.

Figure 5.4: Work environment.

The sound source used was the Norsonic Nor278 (Figure 5.5a), which is typically used for sound power measurements but can also be used for transmission loss measurements as a reference sound source emitting white noise within the source room, in this case the small scale reverberation chamber [57]. The small scale chamber was placed in the center of the hemi anechoic chamber.

The intensity probe used was the PU Regular by Microflown Technologies, which can measure sound pressure and intensity up to 10 kHz (Figure 5.5b). In order to prevent only a portion of the panel from being excited, the reference sound source was positioned so that the generated sound can disperse homogeneously on the measured panel in the incident chamber.

(a)   Sound source.

(b)   Microflown P-U probe.
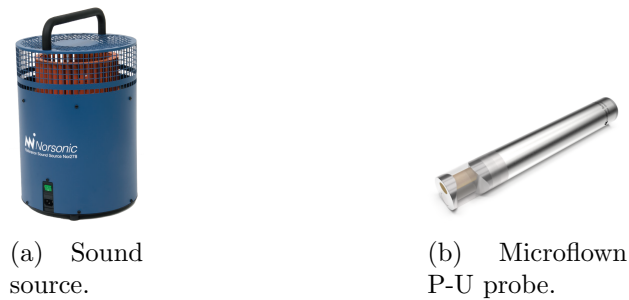
Figure 5.5: Equipment for transmission loss tests.

To prevent sound leaks in the most critical areas of the chamber, butyl was used to cover those same areas, as Figure 5.6 shows. These areas were mainly the interface between the top panel and front and back panels of the reverberation chamber, as it is very challenging to assemble the parts without leaving any gaps between panels. Even the slightest gap can originate a sound leak that affects significantly the results, reducing the achievable transmission loss towards higher frequencies. This part cannot be overlooked and has to be done as carefully as possible.

(a) Back Panel

(b) Front panel

Figure 5.6: Butyl placement in critical areas of the chamber.

The final step to complete the setup was to connect the Scan & Paint video camera, the intensity probe and the Microflown Technologies drivers to a computer containing a Scan & Paint 2D software for sound map visualization (Figure 5.7).
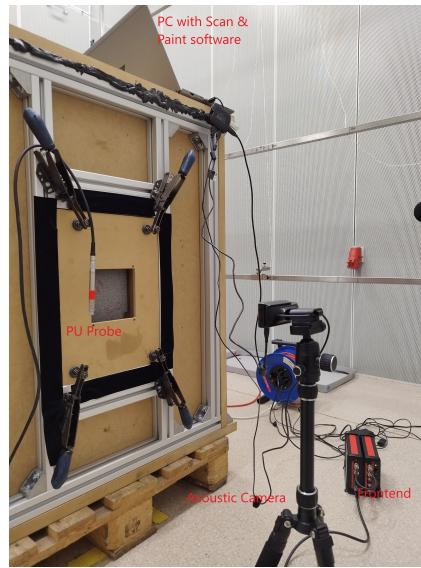
Figure 5.7: Scan & Paint 2D measurements setup.

5.3 Chamber diffusivity

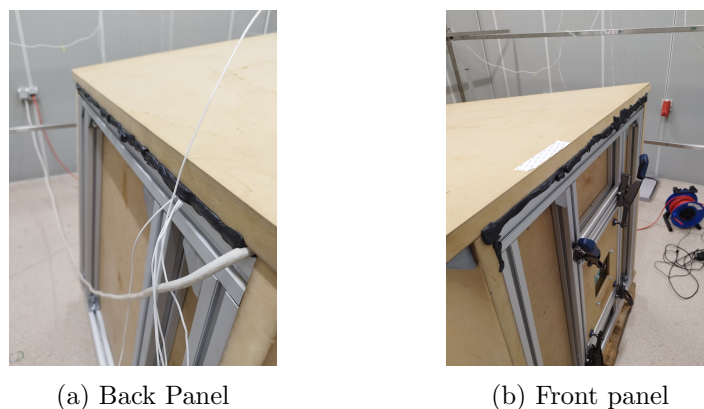In theory, a diffuse sound field should be created within the limits of a reverberation chamber and sound pressure should be the same at any point, regardless of the microphone position in relation to the reference sound source. To check the chamber diffusivity, four microphones were placed in different points of the mini reverberant chamber (Figure 5.8). Naturally, this was done before covering the chamber with the top panel.

(a) Mic setup - tilted back view

(b) Mic setup - front view

Figure 5.8: Microphone setup to test sound diffusivity.

Results validation directly depends on the diffusivity of the chamber. Some tests were performed using different samples, also taking the opportunity to measure the sound pressure level inside the chamber for each sample. Although the sample area is small in comparison to the mini reverberant chamber, sound pressure levels could be slightly affected due to the absorbent characteristics of each foam or geopolymer sample in the bigger scope of the setup.

ArtemiS SUITE, from HEAD Acoustics, was the software used to analyse sound behaviour and evaluate sound pressure levels [58]. It was proven that there were some inconsistencies in diffusivity in frequencies up to 100 Hz, as well as around the frequency range from 200 Hz up to 400 Hz, as shown in Figure 5.9 and Figure 5.10 for two different materials. For the sake of simplicity, only the results obtained from two samples (coloured foam with heavy layer and green foam without heavy layer) are graphically represented.
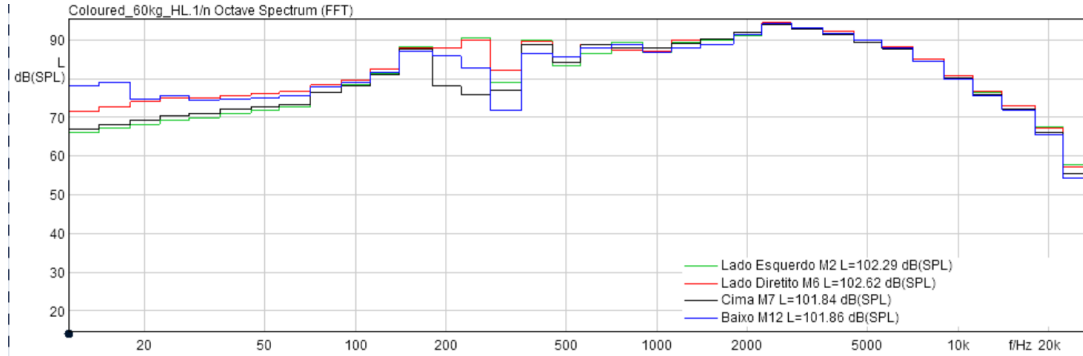
Figure 5.9: Diffusivity test with Coloured agglomerate.
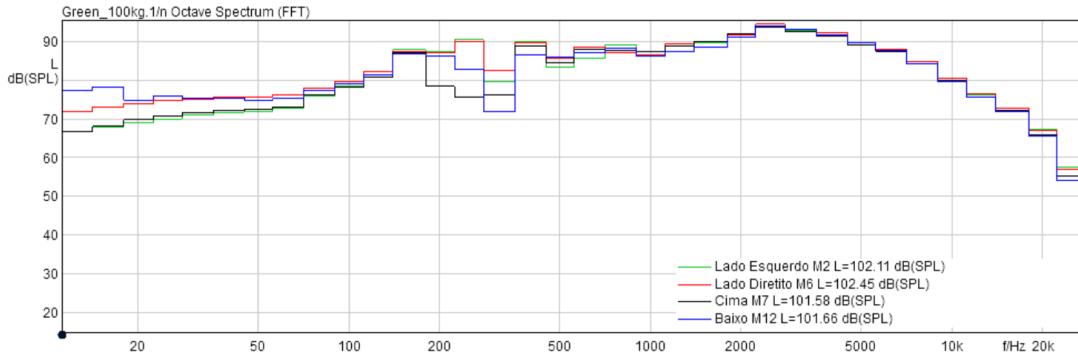
Figure 5.10: Diffusivity test with Green agglomerate.

Discrepancies in the low frequencies may be explained due to the corner frequency of the chamber (f_{corner}=100 Hz), being the minimum frequency from which the chamber shows its anechoic behavior. It is therefore impossible to guarantee that the modes themselves do not dominate the chamber below 100 Hz, having a significant impact on the outcome. Thus, results for sound transmission loss obtained below 100 Hz were evaluated carefully and most time neglected. For sound pressure deviations in the frequencies between 200 Hz and 400 Hz, it can be argued that the chamber itself was not designed in a way that could attenuate the presence of strong dominant waves in this frequency range. A solution to reduce these deviations would be to install diffuser panels to improve sound field diffusivity. Similarly to the low frequencies, sound transmission loss values obtained in the 200 Hz to 400 Hz frequency range have to be carefully analysed, as they may not be entirely reliable.

5.4   Measurements

To conduct the Scan & Paint measurements, each sample was positioned stably on the sample holder to minimize vibrations and undesired side effects. The software used for colour map representation of particle velocity and sound intensity, as well as for extracting the average sound intensity for each frequency throughout most of the 1/3 octave band spectrum was the Velo 5 Scan & Paint 2D, from Microflown Technologies [59]. As recommended by Microflown and in accordance to the pressure-intensity method defined by the ISO 15186-1 standard, sound transmission loss was then calculated by

$$STL = L_p - L_i - 6 \quad (\text{dB}) \tag{5.1}$$

where L_p is the average sound pressure level over the sample panel surface in the source room, in this case being the reverberation chamber. L_i is the average sound intensity level over the sample panel surface in the receiving chamber, in this case the hemi anechoic chamber.

The intensity and velocity maps obtained from the Scan & Paint measurements allowed for the identification of localized sound intensity hot spots or areas with significant variations in sound energy distribution. By examining these maps, valuable insights were gained into the acoustic characteristics of the samples, such as the presence of resonant modes, sound leakage points, or areas of acoustic reflection.

5.4.1   Manually performed tests

The first part of the measurements was done manually. Distance between the p-u probe and the sample plane was kept constant at 50 mm in an attempt to better capture the low frequencies and the orientation of the probe was kept vertical to the sample (Figure 5.11). As indicated in ISO 15186-1, two scans were performed and the scanning pattern was rotated 90$^{\text{o}}$ between scans.
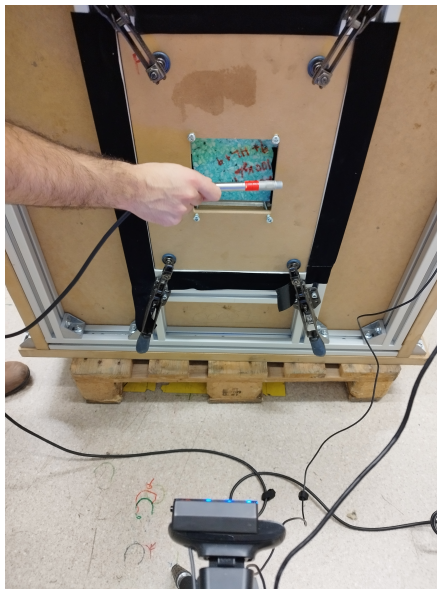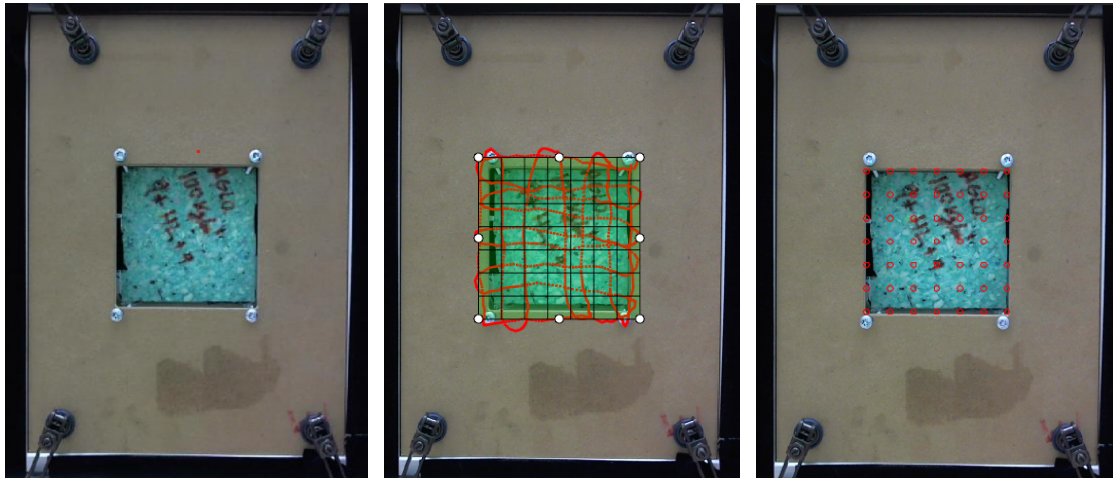

Figure 5.11: Manual Scan & Paint test.

The next stage consisted in processing the data extracted from the measurements. The grid method was chosen for processing every sample, as it is usually faster and allows for better statistical averaged results. This method generates a single value for each grid cell by adding up all measured points within a given grid cell. For exemplification purposes, Figure 5.12 shows the processing steps for the green foam sample with heavy layer and density of 100 kg/m^3.

(a) Pre processing.   (b) Scanning pattern.   (c) Processed data points.

Figure 5.12: Data processing for manual Scan & Paint measurements.

The cells are highlighted in green (Figure 5.12b), proving that the recorded time signal satisfied the provided grid settings and thus enough data can be displayed within each cell. Many times red cells are represented in the grid, indicating that there was not enough data to be displayed due scans faster than desired, and so measurements had to be repeated. The other solution would be to redefine grid settings, increasing the number of cells or extending each block size. However, this can sometimes lead to inaccurate results.

After the data processing, the software presents sound mapping results for the desired frequencies or frequency range. In order to calculate sound transmission loss as requested in the standard, there was a need to analyse, extract and calculate the average sound intensity for each frequency throughout the 1/3 octave band spectrum. Figure 5.13 shows an example of sound intensity mapping for 100 Hz and 5000 Hz.

Even though it is possible to detect leakage in samples using a mapping of sound pressure or intensity, the spatial distribution of the particle velocity has a larger dynamic range, enabling the localisation of weak sound sources. Figure 5.14 shows particle velocity for specific frequencies, proving that it can change drastically depending on the frequency.

Each frequency exhibits a different sound behaviour, but looking at the entire frequency range it is possible to determine where most of the overall leakage is observed. This way one can detect where is the weak point of the sample regarding transmission loss or if the sample was not well isolated before the tests. If the sound map shows many leaks and it is understood that there are no conditions to analyze the results, scanning procedure should be done once again. It should be guaranteed that samples are correctly isolated. Particle velocity sound mapping for the entire range is presented in Figure 5.15.

(a) 100 Hz.   (b) 5000 Hz.
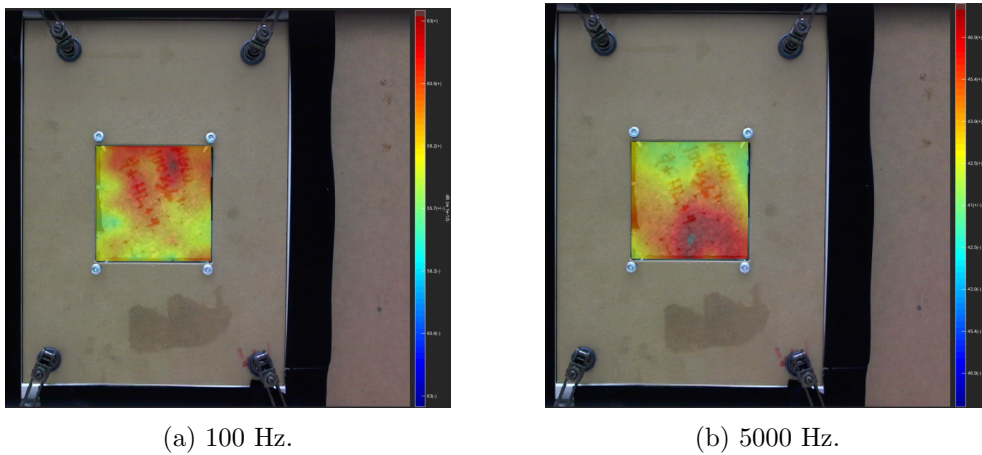
Figure 5.13: Sound Intensity Mapping.

(a) 100 Hz.   (b) 1250 Hz.   (c) 5000 Hz.

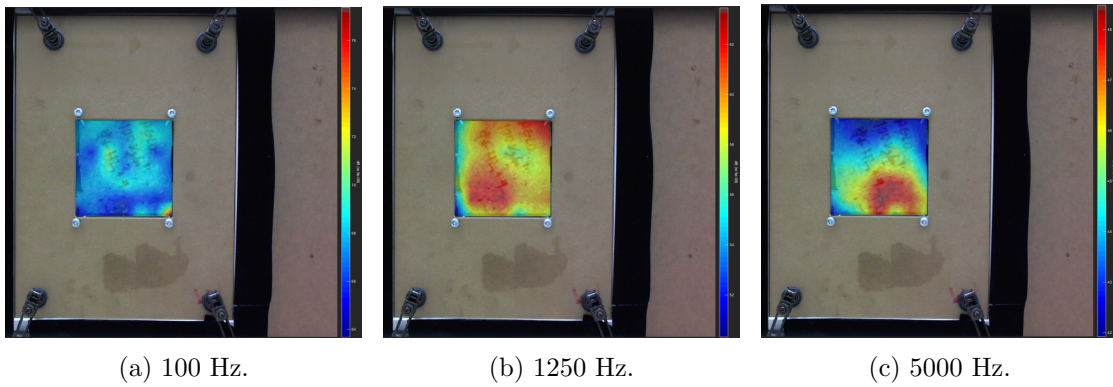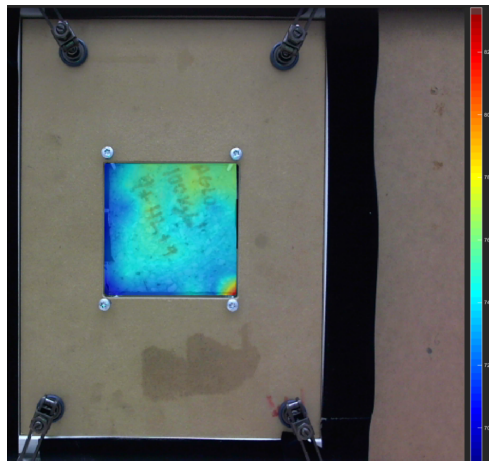Figure 5.14: Particle velocity sound mapping for specific frequencies.

Figure 5.15: Particle velocity sound mapping for the 100 Hz to 5000 Hz frequency range.

Looking at the example of the green agglomerate sample shown in Figure 5.15, it would make sense to better isolate the right lower part of the sample as there is a noticeable leakage in that specific area that could in some way affect transmission loss values.

5.4.2   Automated tests with XY system

As previously mentioned, the automated scanning method was used to ensure consistent and repeatable measurements, reducing human-induced errors and increasing the efficiency of the testing process. Specifically, the automated system was intended to serve four essential purposes:

1. Keep the same speed for the entire duration of the scans.

2. Keep the same distance between the intensity probe and the sample plane for the entire duration of the scans.

3. Keep the probe fixed and the sensor facing the sample plane at all times.

4. Ensure correct orientation of the probe, parallel to the sample, and ensure that the measuring lines are parallel and well distributed in the measuring area.

Then, and aiming to compare results with the manual measurements and to ascertain whether the acquisition of an automatic system for scanning the samples' measurement plane is worthwhile in future works, tests were performed with a XY system in the form of an Ender 3 printing machine. The XY system was programmed to move the sound intensity probe along a predefined grid, covering the entire surface of the sample.
As stated in the previous chapter, the printing machine emits significant noise. To examine the effect of the printer's noise, each sample was tested only with the printer running and without the reference sound source emitting any noise.
Average sound pressure level was measured for each geopolymer and foam sample for the entirety of the scanning routine. This was done since each sample would have an effect on how sound pressure levels are measured by the microphones located in the interior of the small scale reverberation chamber.
Sound transmission loss would then be calculated by

$$STL = L_p - L_{p_{machine}} - L_i - 6 \quad \text{(dB)} \tag{5.2}$$

where L_p is the average sound pressure level over the sample panel surface in the small reverberation chamber. L_i is the average sound intensity level over the sample panel surface in the hemi-anechoic chamber. $L_{p_{machine}}$ is the sound pressure level captured by the microphones inside the reverberation chamber when only the 3D printer is emitting noise, simulating the scanning pattern.
To do this calculation however, it is important to explain how L_p and $L_{p_{machine}}$ must be subtracted. Sound pressure level values in Decibel cannot be changed without first being transformed back into a linear scale. Thus, conversion is done as follows:

$$L_p - L_{p_{machine}} = L_p + \log_{10}(1 - 10^{\frac{-(L_p - L_{p_{machine}})}{10}}). \tag{5.3}$$

Similarly to the manually performed tests, the intensity probe was once again kept at a fixed distance of 50 mm from the samples to better measure low frequencies up to 500 Hz, as recommended in the ISO 15186-1 standard. Scanning speed for both X and Y axis was 55 mm/s. Two scans were performed and the scanning pattern was rotated 90º between scans.
The setup used for the automated measurements is presented in Figure 5.16.
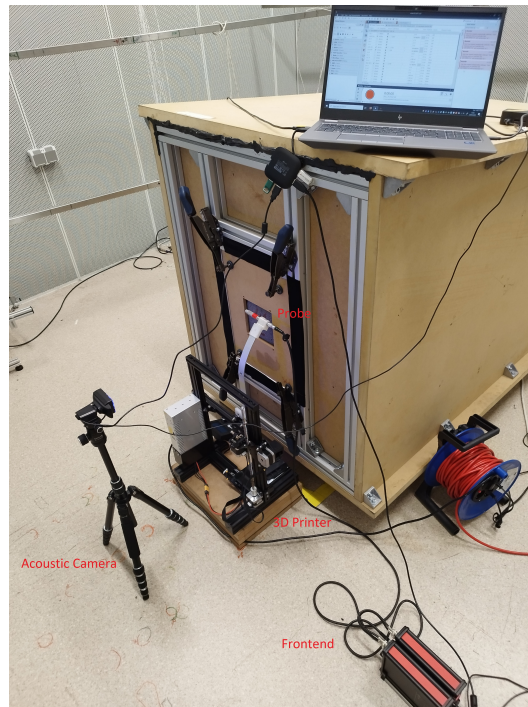
Figure 5.16: Scan & Paint 2D setup for automatic measurements.

An illustration of the probe tracking is presented in Figure 5.17 to better capture the scanning routine, that changed slightly in comparison to the manually performed scans as a result of stock firmware limitations. As it can be seen, in the edges at the end of each scanning line, the semi circular approach was replaced by an angular pattern. Regarding data processing, the grid method was also used for this analysis due to better statistical averaged results. Steps are illustrated in Figure 5.18.

(a)   (b)
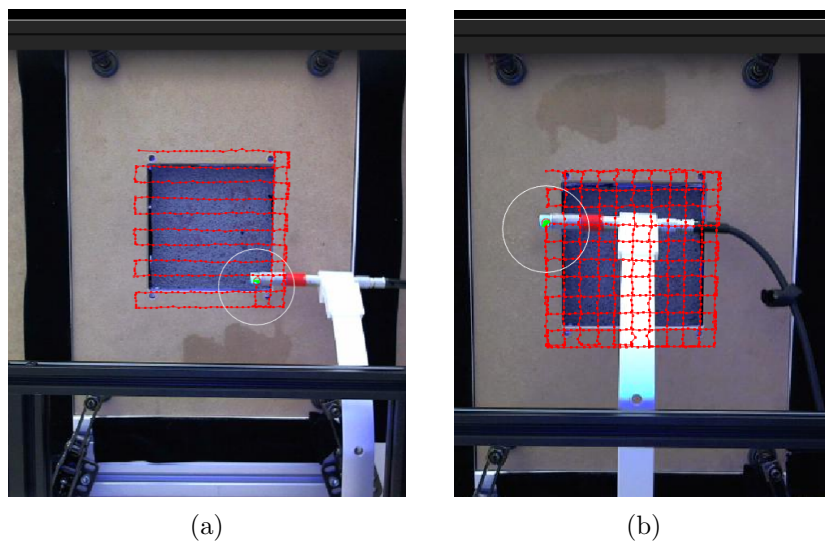
Figure 5.17: Probe tracking.

(a) Scanning pattern.   (b) Processed data points.
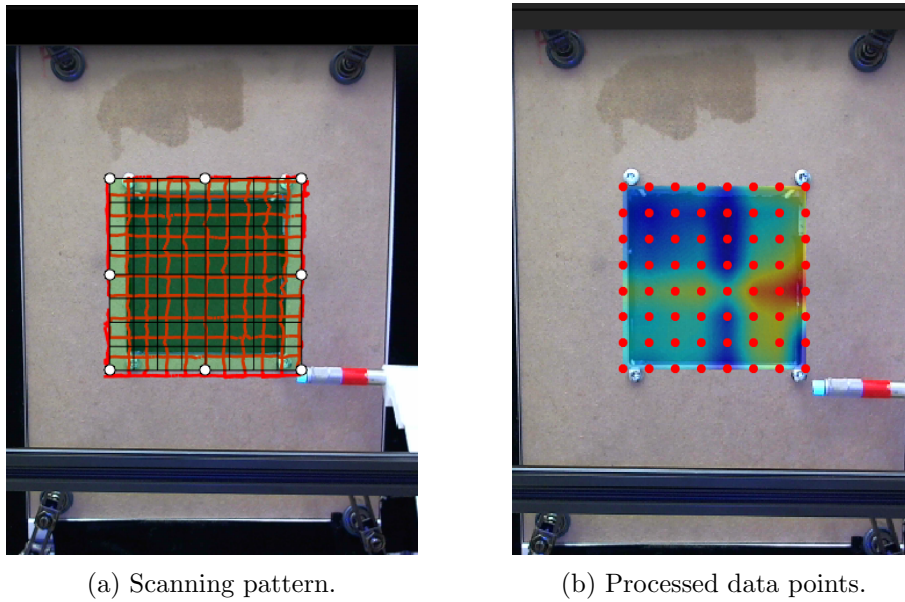
Figure 5.18: Data processing for automatic Scan & Paint measurements.

At this stage it is important to compare both methods to confirm that the color maps are similar, indicating that there was a degree of uniformity, at least regarding the measurement of sound intensity.

Once again, for exemplification purposes, Figures 5.19, 5.20, 5.21 and 5.22 show how sound intensity mapping compare on both methods, for a low frequency and a high frequency, in different samples.

For each figure, the sample on the left was scanned manually, while the one on the right was scanned with the automatic system.
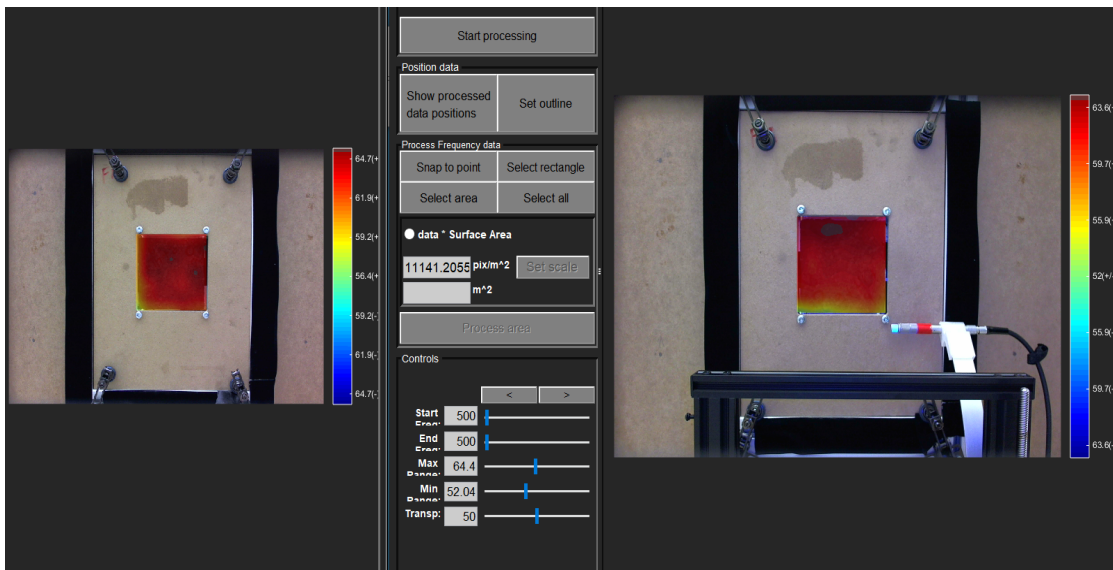
Figure 5.19: Intensity mapping for Black agglomerate with heavy layer (500 Hz).
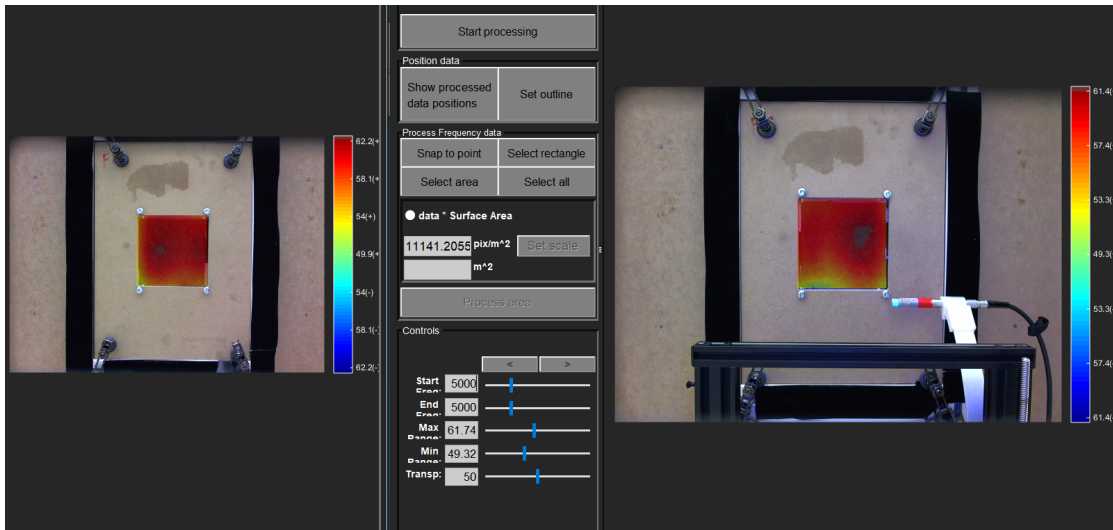
Figure 5.20: Intensity mapping for Black agglomerate with heavy layer (5000 Hz).
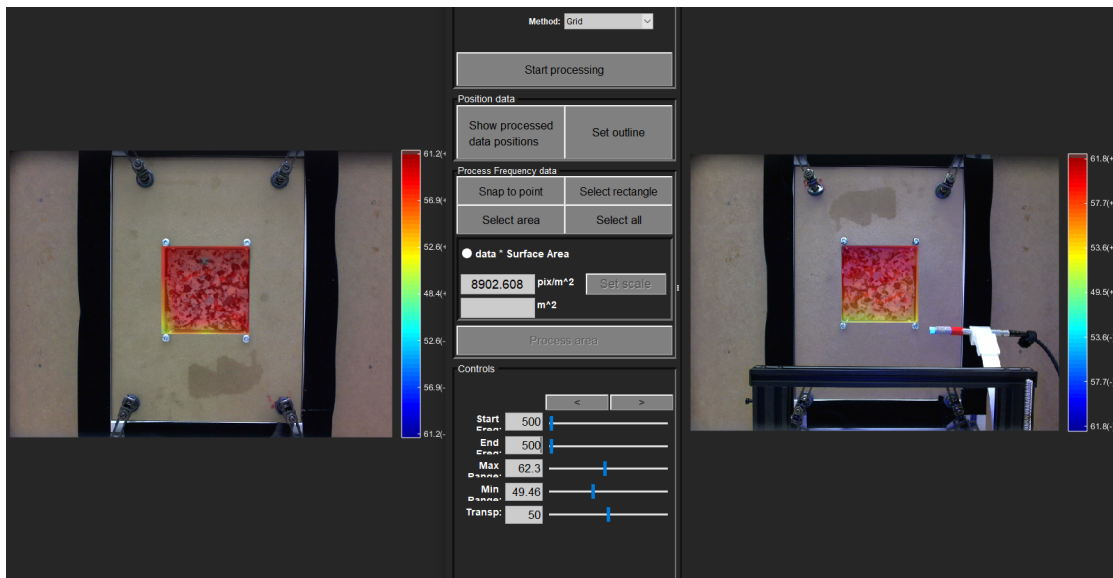
Figure 5.21: Intensity mapping for Coloured agglomerate with heavy layer (500 Hz).

Spatial distribution of sound intensity does not vary significantly with frequency, suggesting that the samples may possess homogeneous acoustic properties, resulting in a consistent sound intensity distribution regardless of the frequency.

Also, the consistent sound intensity color map observed across frequencies can indicate that the samples may not exhibit prominent resonant modes within the tested frequency range.

Bonded foam and geopolymers have relatively uniform structures throughout their composition. This uniformity can lead to consistent sound intensity patterns since the sound waves encounter consistent material properties as they propagate through the samples. It indicates that the materials have consistent acoustic behavior and do not exhibit significant variations in sound absorption or reflection characteristics with frequency.
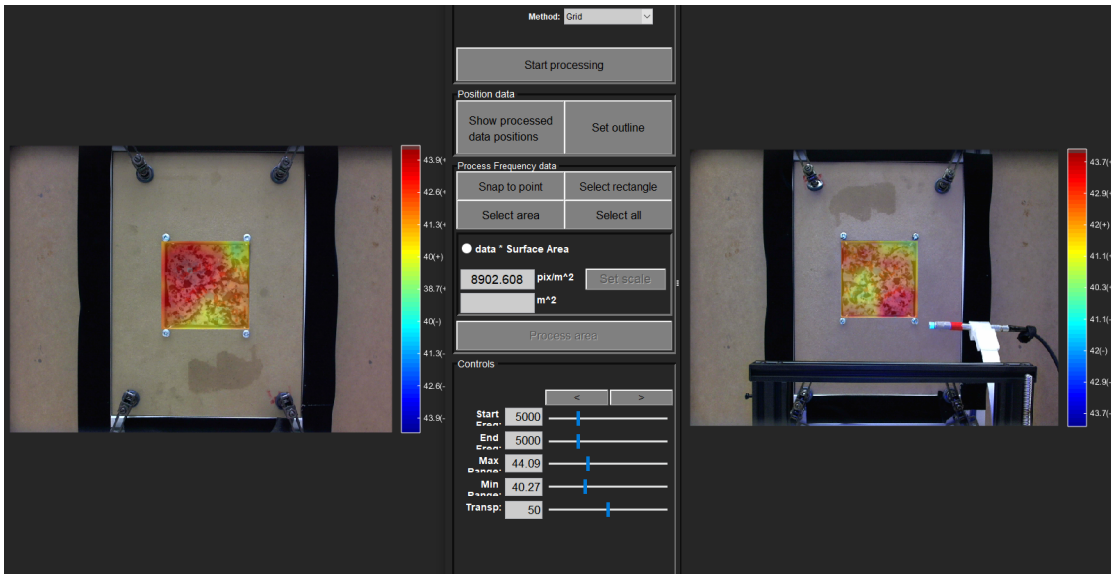
Figure 5.22: Intensity mapping for Coloured agglomerate with heavy layer (5000 Hz).

However, it was observed a discrepancy in some geopolymer samples. In the low frequency range, specially at 100 Hz, automatic measurements results differed considerably from the manual ones, as shown in Figure 5.23.
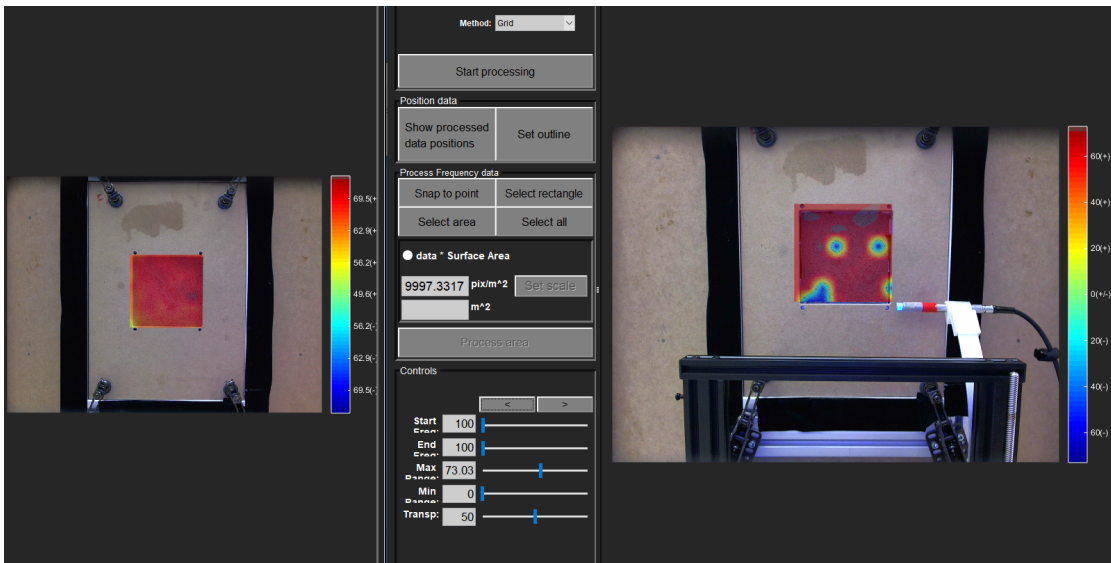
Figure 5.23: Intensity mapping for a 20 mm geopolymer sample with 0.15% aluminium.

In the context of these tests, it is expected for sound intensity to have a uniform distribution across the sample plane. The geopolymer shown in Figure 5.23 is exactly the same on both sides, thus the manual and automatic measurement methods have different sensitivities at 100 Hz compared to other frequencies. It is possible that the manual method is more capable of accurately capturing sound intensity variations at 100 Hz, while the other may exhibit reduced sensitivity or accuracy at that or similar frequencies.

Chapter 6

Results and Discussion

The results obtained from the experiments conducted to compare the sound transmission loss of different materials are presented in this chapter. Data was analysed and grouped in specific ways to determine the effectiveness of each material in reducing sound transmission. All samples were tested in the same conditions, although there's certainly the possibility of inconsistent speed and distances between the sample and the measuring sensor in the manually performed scans. However, results should be analysed as though measurements were executed homogeneously.

6.1 Manual tests

6.1.1 Sound transmission loss of foam samples

The results are analysed within the frequency spectrum from 100 Hz to 5000 Hz. Figure 6.1 presents results regarding the acoustic performance of foam samples with bitumen heavy layer.

Figure 6.1: Sound transmission loss of foam samples with heavy layer.

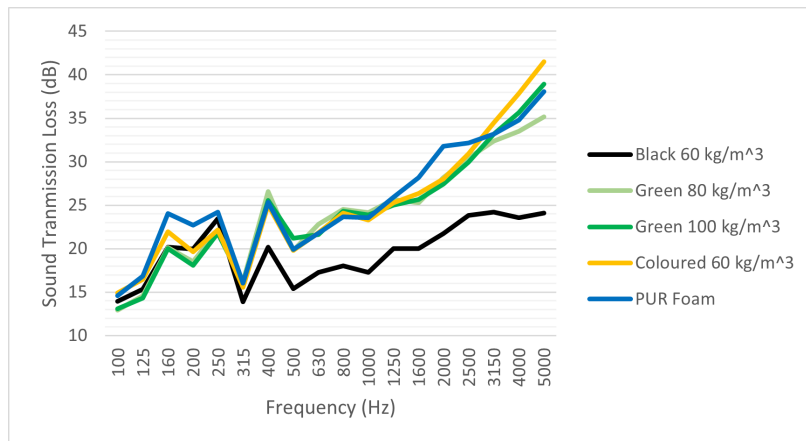Analysing samples with the presence of heavy layer may show its impact on sound insulation properties of the materials. It is important to note that curves from all samples follow the same trend, although conclusive results were not reached regarding the effects

of density in this case. For instance, above 2500 Hz, the coloured bonded foam showed higher values of transmission loss, despite its lower density compared to other samples. From 315 Hz onwards, the black agglomerate proves to be the weakest performer and the green agglomerates show practically equal values of transmission loss throughout the frequency spectrum, apart from the higher frequencies. In the low frequencies, PUR foam is the best sound insulator, which is surprising as in theory this material is known to be a better performer at higher frequencies. The high density and greater thickness in the PUR foam sample might explain the better results at lower frequencies.

Figure 6.2 shows the performance without the presence of heavy layer.
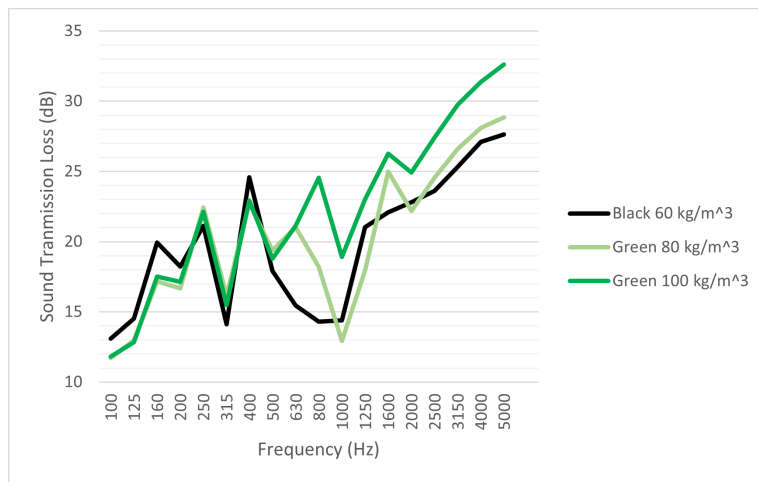
Figure 6.2: Sound transmission loss of foam samples without heavy layer.

The removal of hard layer indicates that higher density agglomerates perform better, except in the low frequencies up to 200 Hz and in some specific frequencies such as 400 Hz and from 1000 Hz up to 1600 Hz, though difference does not even reach 3 dB.

Other observations can be made grouping agglomerates of the same type. Figure 6.3 and Figure 6.4 present the sound transmission loss of the isolated green and black agglomerates, respectively.
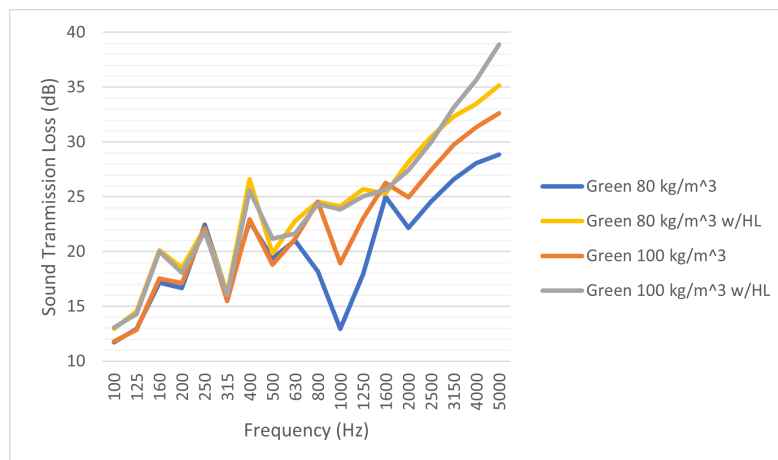
Figure 6.3: Sound transmission loss of green foam agglomerates.
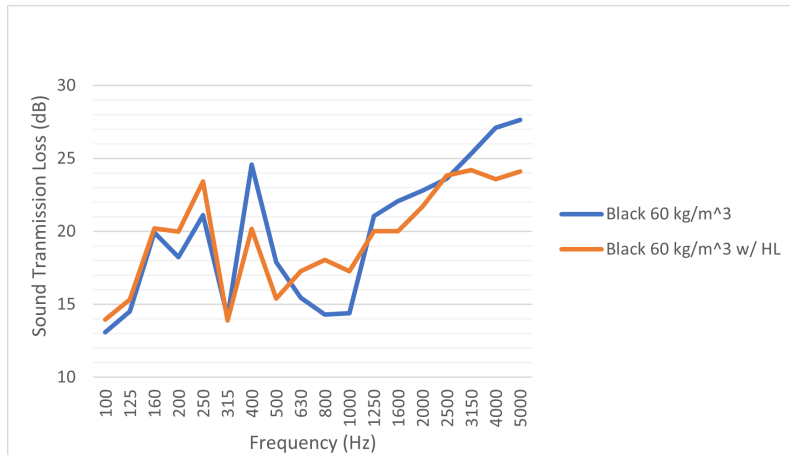
Figure 6.4: Sound transmission loss of black foam agglomerates.

For the green agglomerate, samples containing heavy layer present higher transmission loss values. Density practically has no effect in transmission loss up to 3150 Hz in samples containing heavy layer, but increases the insulation performance once the hard layer is removed from 630 Hz onwards. On the other hand, results for the black agglomerate are inconclusive in regards to the presence of heavy layer. In the low frequencies up to 315 Hz and between around 630 Hz and 1250 Hz, the presence of heavy layer shows higher values of transmission loss, although surprisingly in the rest of the frequency spectrum up to 5000 Hz its presence translates into a reduced acoustic performance.

Performance of foam samples in a broader scope for the entirety of the frequency range can be examined as well. The method used splits the area between the curve and x axis to multiple trapezoids, calculates the area of every trapezoid individually and then sums up these areas. According to this criteria, the curve that forms the bigger area should indicate the overall best sound insulator, as shown in Table 6.1 below.

Table 6.1: Overall acoustic performance of foam samples.

Sample	Overall Performance - Area Units
Black 60 kg/m^3	113285.4
Black 60 kg/m^3 w/HL	107119.8
Coloured 60 kg/m^3 w/HL	151872.1
Green 80 kg/m^3	117401.0
Green 80 kg/m^3 w/HL	142978.0
Green 100 kg/m^3	132016.4
Green 100 kg/m^3 w/HL	146502.6
PUR	149953.4

The coloured agglomerate proves to be the material with the overall higher sound transmission loss. There are better acoustic performances with the presence of heavy layer, except for the black agglomerate. Apart from the coloured foam, an increase in density results in higher transmission loss as well. It was also proven that PUR can very much compete with other foams for sound proofing applications, if enough density is applied.

6.1.2   Sound transmission loss of geopolymers

For geopolymers, it is interesting to study results at higher frequencies due to little data and thus, frequencies up to 10000 Hz were analysed.

Figure 6.5 and Figure 6.6 show the sound transmission loss of geopolymer samples with 0.10% and 0.15% aluminium, respectively.
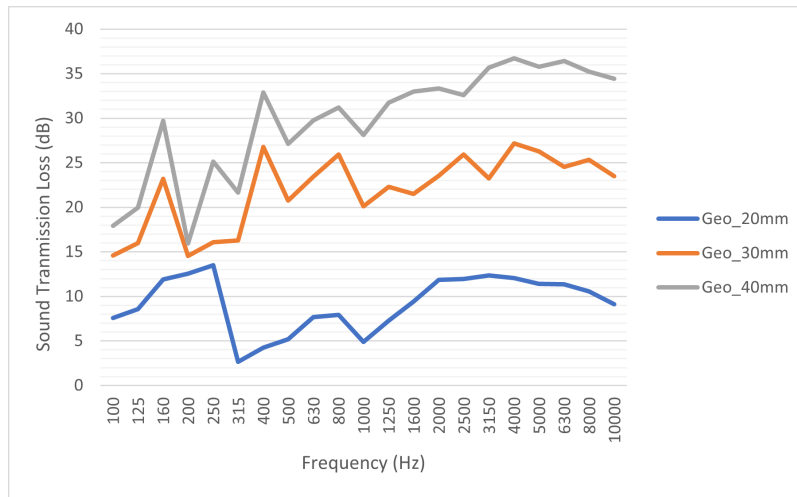
Figure 6.5: Sound transmission loss of geopolymers with 0.10% aluminium.
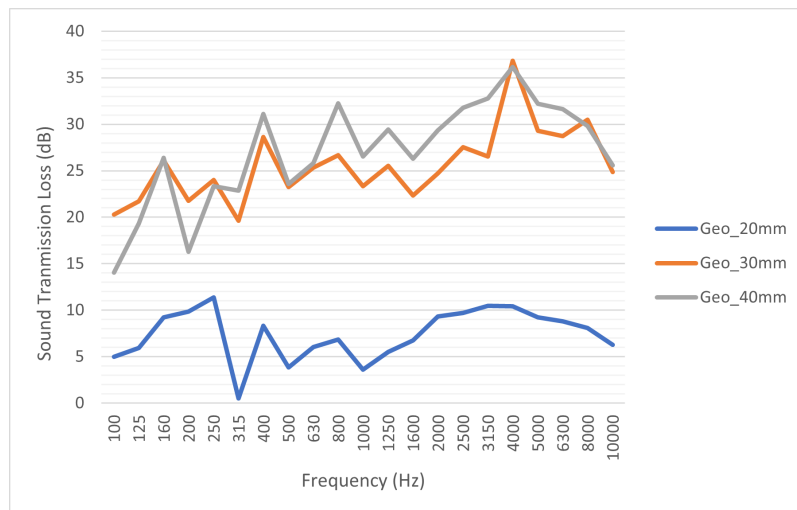
Figure 6.6: Sound transmission loss of geopolymers with 0.15% aluminium.

For geopolymers with 0.10% aluminium there is a clear improvement in transmission loss when the sample thickness is increased for all frequencies. Curves for 30 mm and 40 mm samples follow basically the same tendency, where transmission loss peaks at 160 Hz and 400 Hz in lower frequencies and slightly decreases from 4000 Hz up to 10000 Hz. The 20 mm sample proves to be much less effective for sound proofing, peaking at 250 Hz with a transmission loss of only around 14 dB. From 2000 Hz onwards there is stagnation and even a small decrease in the transmission loss towards 10000 Hz.

As for geopolymer samples with 0.15% aluminium, there is an indication that sound behaviour is not so linear. Despite the similarity in the tendency of the curves in the 30 mm and 40 mm samples, the former shows slightly better transmission loss values at low frequencies up to 250 Hz. Peaking at 4000 Hz with 37 dB, the 30 mm sample is actually the one with the highest value of sound transmission loss throughout the frequency spectrum. Values observed for 30 mm and 40 mm samples suggest that thickness may play a lesser role in sound transmission loss when increasing the aluminium content, at least above 30 mm. Nevertheless, the 20 mm sample shows poor acoustic performance, with values similar to its counterpart with 0.10% aluminium.

Just like for the foam samples, a general overview analysis was conducted, presented below in Table 6.2.

Table 6.2: Overall acoustic performance of geopolymer samples.

Sample (thickness)	Overall Performance - Area units
Geopolymer 0.10% Al. (20mm)	104106.7
Geopolymer 0.10% Al. (30mm)	242294.9
Geopolymer 0.10% Al. (40mm)	340248.3
Geopolymer 0.15% Al. (20mm)	82363.2
Geopolymer 0.15% Al. (30mm)	280015.5
Geopolymer 0.15% Al. (40mm)	300286.8

Overall, these results prove that an increase in thickness translates into higher values of sound transmission loss for both types of geopolymer samples. Results from two out of three samples (20 mm and 40 mm) also indicate that lower contents of aluminium that ultimately translate into denser and less porous specimens might improve transmission loss. However for the 30 mm samples the opposite was verified. Thus, at this stage it is quite difficult to draw conclusions regarding the effects of aluminium content in samples with lower thickness, although generally it still can be said that sound transmission loss improves when density is increased.

6.2   Automated tests

6.2.1   Sound transmission loss of foam samples

Acoustic performance of foam samples containing bitumen heavy layer are presented in Figure 6.7. Once more, the curves follow somewhat the same trend throughout the frequency range. This method also confirms the inconclusive nature of density in sound transmission loss. At high frequencies, the coloured agglomerate has the best acoustic performance. The black agglomerate proves once again to be the worst material from 315 Hz onwards and the PUR foam continues to show great acoustic capabilities.

Figure 6.8 shows the sound transmission loss for samples without heavy layer. Here, curves from the green agglomerates follow the same trend. It can be noticed a slight improvement in transmission loss from 630 Hz onwards when density is increased. However, in the low frequencies the low density black agglomerate presents transmission loss values hugely different from the ones shown by the green agglomerates, even though the latter have higher densities.
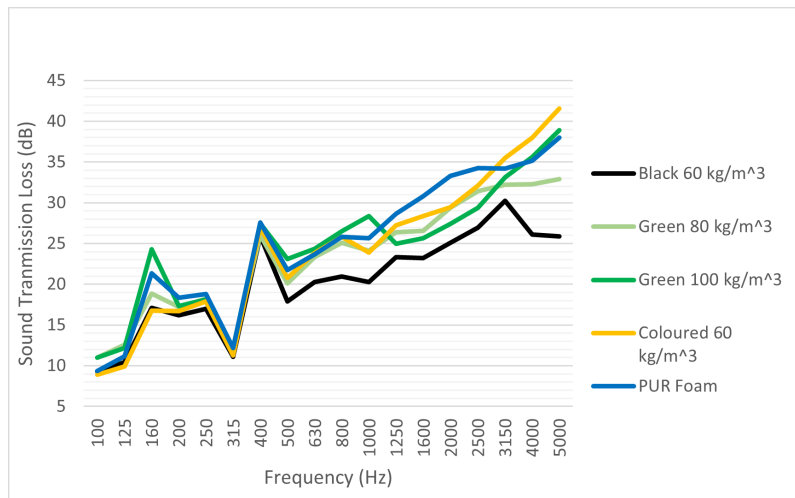
Figure 6.7: Sound transmission loss of foam samples with heavy layer.
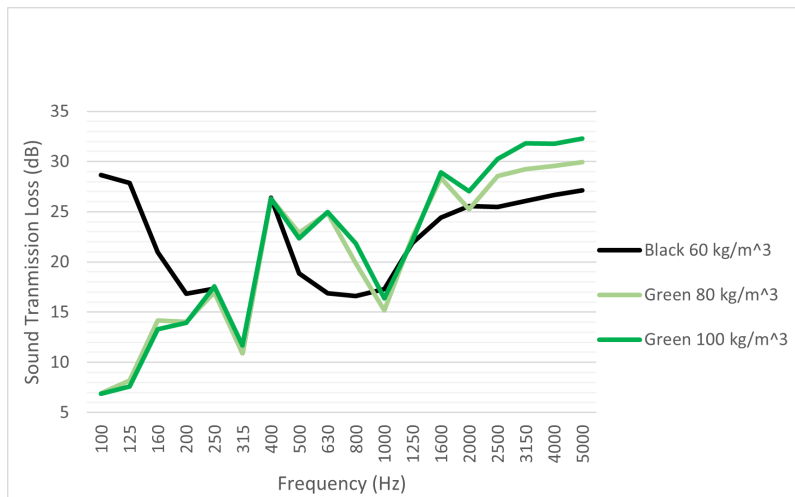
Figure 6.8: Sound transmission loss of foam samples without heavy layer.

Figure 6.9 and Figure 6.10 show sound transmission loss for the green and black agglomerates, respectively.

Regarding the green agglomerates, the presence of a heavy layer generally seems to increase the sound transmission loss, except in the range between 400 Hz and 630 Hz and especially at 1600 Hz. Sound transmission loss seems to be specially improved in the low frequency range up to 250 Hz when the bitumen heavy layer is present in the samples. As for the black agglomerates, results are once again inconclusive regarding the presence of heavy layer. In the low frequency range from 100 Hz to 250 Hz there is a significant difference between both samples. The sample without bitumen heavy layer actually shows much higher sound transmission loss, contrary to what might have been expected. Then, from 250 Hz up to 500 Hz, sound transmission loss is practically the same on both samples. From 500 Hz onwards, there are several segments throughout the frequency spectrum where either the existence or the non-existence of heavy layer show higher values of sound transmission loss.
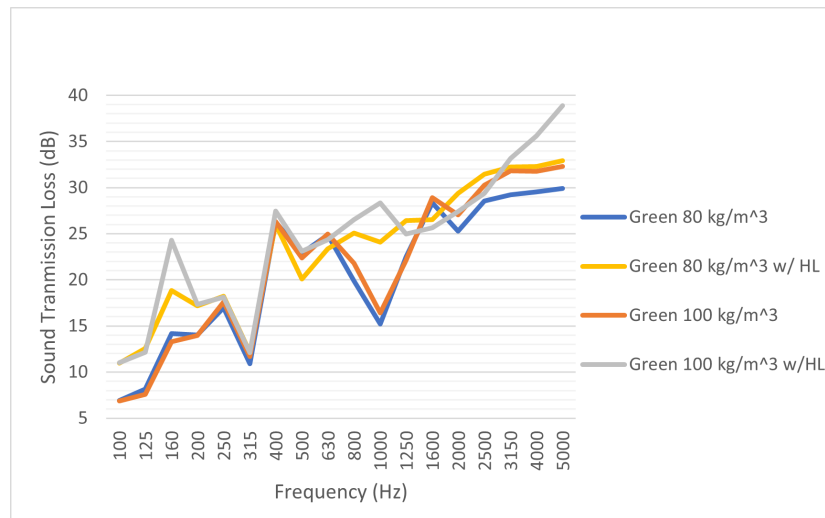
Figure 6.9: Sound transmission loss of green foam agglomerates.
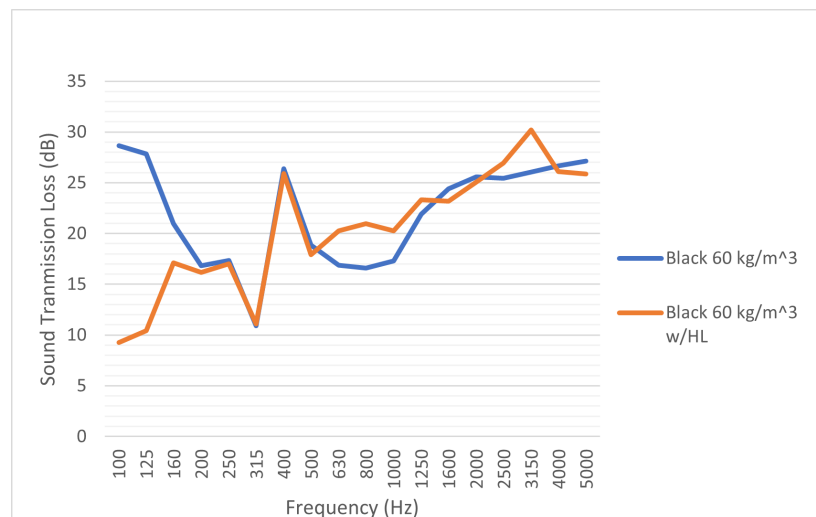
Figure 6.10: Sound transmission loss of black foam agglomerates.

An overview of the acoustic performance from all foam samples is shown in Table 6.3. This analysis indicates that the coloured foam is the material showing greater acoustic performance. There is a clear improvement in sound transmission loss when the sample presents a heavy layer attached to the foam layer. When density increases, materials exhibit higher soundproofing capabilities. As for the PUR foam, sound transmission loss results are once more quite good compared with the rest of the samples, being the second best sound insulator. However, it once again worth recalling that the considerable thickness of the sample aligned with high density of the PUR foam is considered to be the main factor as to why it is so competitive as a sound insulator, and especially at the low frequency range.

Table 6.3: Overall acoustic performance of foam samples.

Sample	Overall Performance - Area Units
Black 60 kg/m^3	118331.9
Black 60 kg/m^3 w/HL	121757.6
Coloured 60 kg/m^3 w/HL	155328.9
Green 80 kg/m^3	128557.0
Green 80 kg/m^3 w/HL	141901.7
Green 100 kg/m^3	136238.3
Green 100 kg/m^3 w/HL	147872.1
PUR	155175.9

6.2.2   Sound transmission loss of geopolymers

Figure 6.11 and Figure 6.12 present the sound transmission loss of geopolymer samples with 0.10% and 0.15% aluminium, respectively.

For the case of geopolymers with 0.10% aluminium, the similarity in values throughout the entire frequency range may suggest that thickness does not affect transmission loss values in a significant manner. However, at frequencies above 5000 Hz it can be seen improvements in acoustic performance as the thickness is increased.

On the other hand, geopolymer samples with 0.15% and 40 mm thickness show higher sound transmission loss values in all frequencies compared with the ones with thicknesses of 20 mm and 30 mm. Regarding the latter, the effect of thickness is quite inconclusive as samples with 20 mm and 30 mm since one overlaps the other and vice versa in terms of transmission loss values depending on the frequency. One major remark from these results is the surprisingly good sound transmission loss values up to 250 Hz of the 40 mm thick sample, hitting as high as 24 dB at 100 Hz.

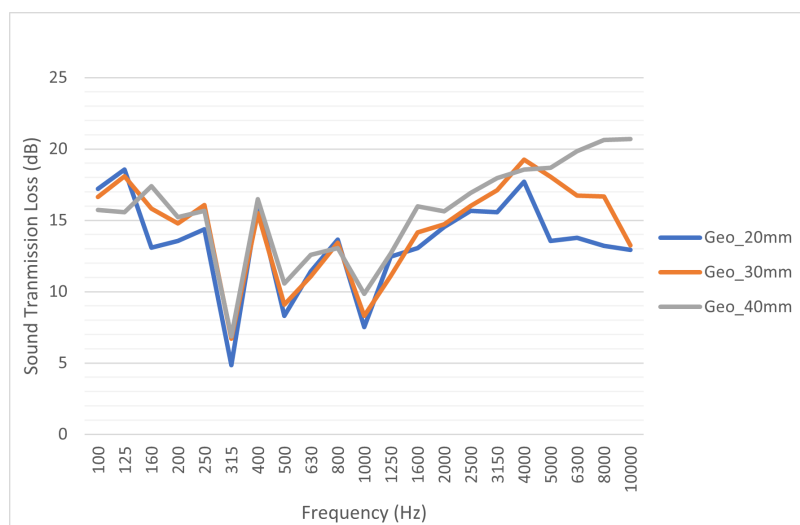Table 6.4 presents the overall acoustic performance of geopolymer samples.

Figure 6.11: Sound transmission loss of geopolymers with 0.10% aluminium.
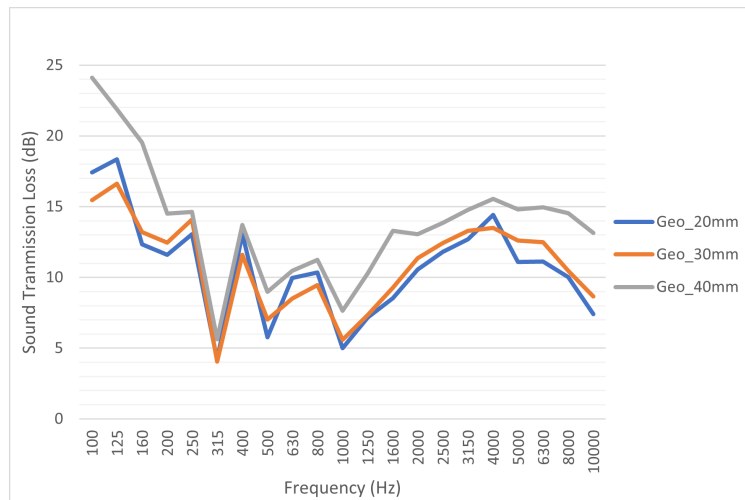
Figure 6.12: Sound transmission loss of geopolymers with 0.15% aluminium.

Table 6.4: Overall acoustic performance of geopolymer samples.

Sample (thickness)	Overall Performance - Area units
Geopolymer 0.10% Al. (20mm)	137248.3
Geopolymer 0.10% Al. (30mm)	156919.0
Geopolymer 0.10% Al. (40mm)	179979.3
Geopolymer 0.15% Al. (20mm)	104284.1
Geopolymer 0.15% Al. (30mm)	110672.3
Geopolymer 0.15% Al. (40mm)	138157.9

This general overview indicates that the increase in thickness also increases the overall acoustic performance of the samples, regardless of their aluminium content. It also proves, for the tested samples, that the lower the aluminium content, the better the transmission loss for all samples.

6.3   Comparison between manual and automatic tests

The objective of this section is to compare results from both methods and assess the reliability of the automatic method.

6.3.1   Difference in sound transmission loss

Manual tests are known to be reliable as they are supported by the literature and are performed frequently in industrial applications to evaluate sound behaviour of the most diversified equipment. Measurements with small scale reverberation chambers placed inside anechoic environments have also been performed with trustworthy results, as previously mentioned in Chapter 2. For the automatic measurements, reliability is yet to be proven. Figure 6.13 and Figure 6.14 show the difference in sound transmission loss between the manual and automatic tests for foam and geopolymer samples, respectively.
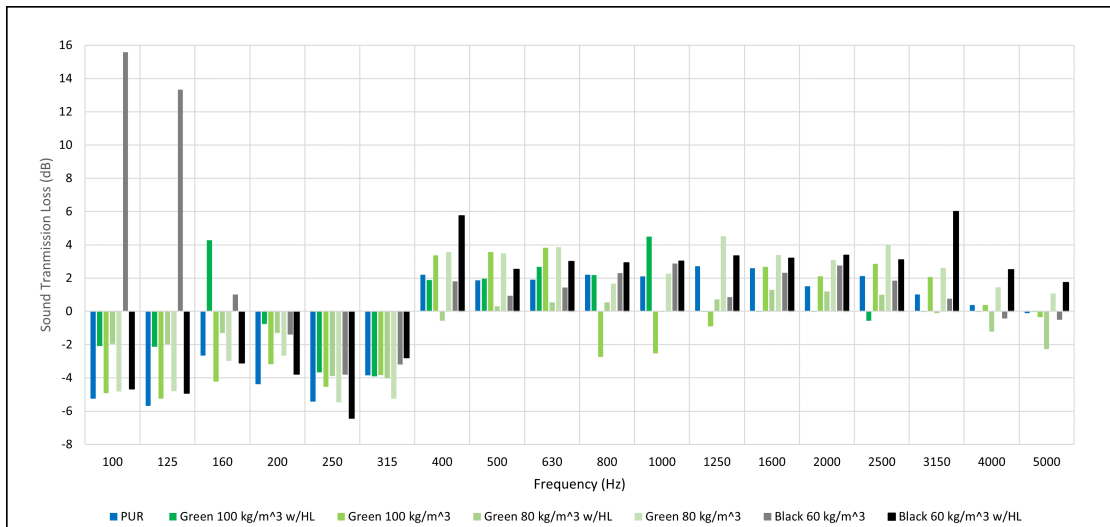
Figure 6.13: Sound transmission loss difference for foam samples.
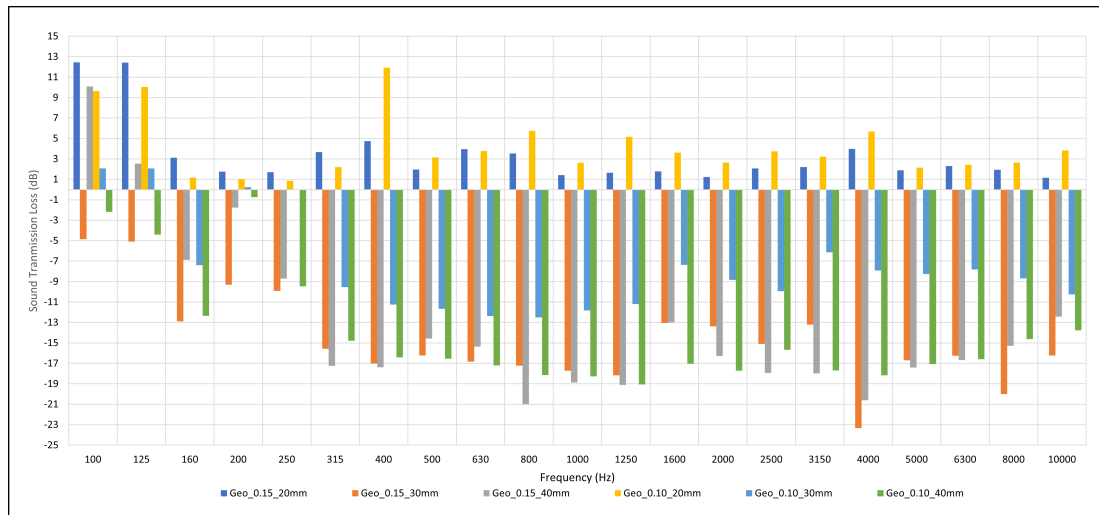
Figure 6.14: Sound transmission loss difference for geopolymer samples.

Upon analyzing the results obtained from both the manual and automatic tests, notable differences in sound transmission loss were observed, particularly in the geopolymer samples and in one specific low density bonded foam agglomerate (Black 60 kg/m^2). The discrepancies were most pronounced at certain frequencies, with variations surpassing 20 dB between the manual and automatic tests in some geopolymer samples. This is not ideal to assess the reliability of the results, specially for the measurements performed with the automated system. However, differences in foam samples are not so pronounced, except for the mentioned case of the black agglomerate.

6.3.2 Reliability of automatic test results

Tests with equal samples

As for the measurements themselves, the automatic procedure was performed with the same routine for every sample and in the same conditions of the manual tests.

Since results from the previous measurements were quite unexpected, some others were performed to access the uniformity of the automatic test results. It was measured the sound transmission loss of three equal 29 mm thick geopolymer samples and three equal 41 mm thick geopolymer samples. Results are shown in Figure 6.15 and Figure 6.16.

The repeatability of the tests was not quite ensured with the automatic tests, even though there was achieved a precise distance and positioning of the measurement probe in relation to the sample plane. The scanning speed was the same for all measurements and the orientation of the probe was kept parallel to the sample plane at all times, avoiding vibrations and other influences.
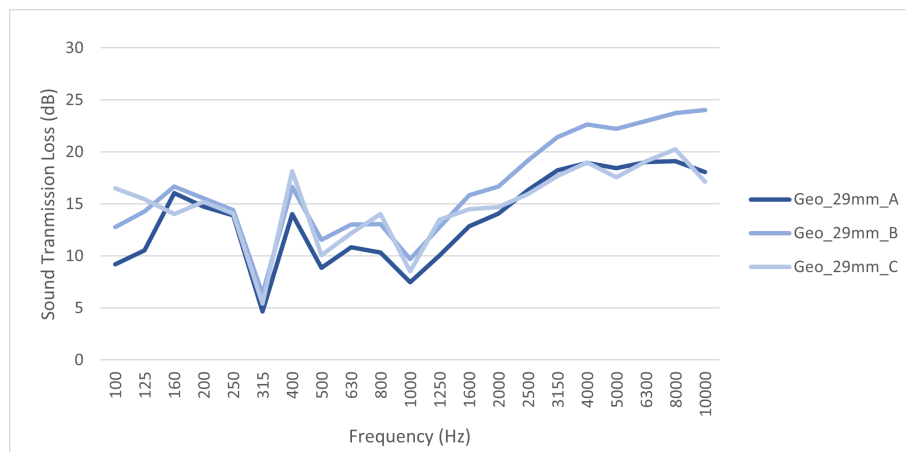

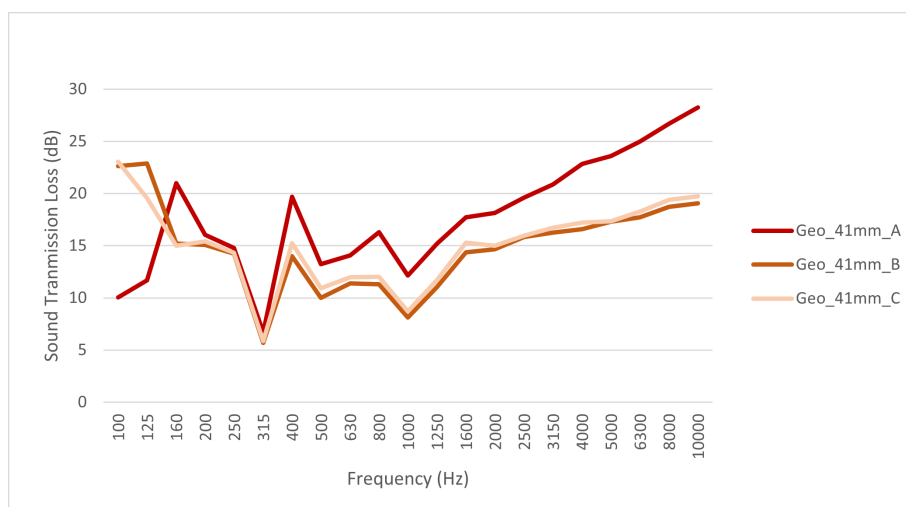Figure 6.15: Sound transmission loss of 29 mm thick geopolymer samples.

Figure 6.16: Sound transmission loss of 41 mm thick geopolymer samples.

It is suggested that even though transmission loss values in some frequencies showed good agreement across all tested samples, the uniformity of the testing procedure did not translate into uniformity of results throughout the whole frequency spectrum. This is especially noticeable in the low frequencies and from 1600 Hz onwards.

Automatic test measurements clearly have different sensitivities or limitations compared to the manual method. The latter seems to be more capable of accurately capturing sound intensity variations at lower frequencies while the other method may exhibit reduced sensitivity or accuracy in those frequencies.

Considerations about the use of the automatic method

Results from figures 6.15 and 6.16 indicate that all curves follow a similar trend from 160 Hz onwards, which makes sense as all samples are equal and have practically the same acoustic behaviour.

Thus, for the automatic method, conducting multiple scans for each sample and subsequently averaging the results can help mitigate the effects of measurement inconsistencies and enhance the accuracy of the sound transmission loss results. This approach can provide a more representative picture of the sample acoustic behavior but would take away the main goal of using the automatic method, which is the efficiency of the tests. Sound transmission loss results for bonded foam and geopolymer samples were not obtained following this process due to time limitations.

Human error has to be taken into account when manual tests are performed, however the automatic procedure used in this work was not able to compensate the imprecision of regular testing procedures.

The main factors that may have contributed to the great disparity in some transmission loss results between the automatic and manually performed testes may have been:

- Loss of anechoic conditions in the receiving side as a result of the physical contribution of the aluminum profiles that make up the 3D printer, as well as the profile that supports the probe, among other components. These are highly reflective and for the purposes of this study could be seen as diffusers, and could even have created a diffuse sound field in a small spatial frame around the sample plane.

- Imprecision with the formula used to calculate sound transmission loss in the automatic method, as it may need a calibration factor to better predict the results related to the external component that assists in the measurements and that in the process emits some undesired noise (the 3D printer).

As for individual measurements, frequencies closer to the hemi anechoic chamber cutoff frequency (100 Hz) can be susceptible to inaccurate measurements due to a possible dramatic loss of free field conditions. Also, the lack of diffusivity in the source chamber from 200 Hz to 400 Hz may explain the results observed in that specific range, as explained previously.

In the end, it would be somewhat risky to rely completely on the results obtained through the automatic method. Therefore, in light of this work, results of the acoustic performance of materials to be considered for heat pump structural incorporation should be those obtained by the manual method.

Chapter 7

Conclusion

7.1 Application of tested materials in heat pumps

Heat pumps play a crucial role in various applications, including residential and commercial heating, ventilation, and air conditioning systems. The integration of appropriate materials within heat pump components can significantly impact their performance, efficiency, and noise characteristics. The sound transmission loss properties of materials used in heat pump systems are of utmost importance to ensure optimal acoustic performance. The tested bonded foams and geopolymers demonstrate promising sound transmission loss values. The utilization of bonded foams and geopolymers in heat pump components can contribute to noise reduction and improve acoustic comfort.

Overall, the tested materials can be applied as vibration-damping layers, gaskets, or seals in compressor housings, air ducts, and expansion valves.

However, for acoustic purposes, bonded and PUR foams are normally used for Industrial Design Covers (IDC), which are the insulation materials for heat pump enclosure plates, as shown in Figure 7.1a.

Since the compressor is one of the components that produces most of the noise, foam materials are also used for compressor insulation, commonly referred as compressor jackets. Compressor jackets are designed to mitigate noise by providing sound insulation around the compressor unit. They effectively create a barrier between the compressor and its surroundings. Generally, even though compressor insulation may attenuate noise above 500 Hz, it could also amplify it in lower frequencies due to greater vibrating surface area, especially if realized with stiffer materials. So, the use of these insulations have to be studied carefully. Compressor jackets can provide some additional advantages besides only lowering noise. They give the compressor insulation, shielding it from temperature changes outside and possibly enhancing its energy efficiency. Compressor jackets can assist prevent condensation or frost formation on the compressor by reducing exposure to cold temperatures, ensuring the compressor operates at its best. Figure 7.1b shows a detail of a compressor jacket concept.

Their viscoelastic properties can effectively attenuate vibration and reduce structure-borne noise transmission, thereby minimizing the overall noise level emitted by the heat pump system.

Apart from their acoustic benefits, the tested materials also hold the potential to enhance the energy efficiency of heat pumps. The use of bonded foams and geopolymers can reduce heat losses during the operation of heat pumps, resulting in improved overall

system efficiency. The low thermal conductivity and high insulation properties of these materials help minimize energy wastage, leading to reduced operational costs and low environmental impact.

The durability and longevity of materials applied in heat pumps are essential considerations. The bonded foams and geopolymers exhibit excellent resistance to moisture, chemicals, and temperature variations, making them suitable for long-term use in heat pump systems. Their robustness and dimensional stability contribute to the overall reliability and extended lifespan of the heat pump components as well.

(a) IDC.   (b) Compressor jacket.

Figure 7.1: Insulation details in heat pump applications.

7.2   Overview

In this work, the main focus was to compare materials typically applied in heat pumps for sound insulation. Two types of materials were tested, bonded foam and geopolymers, and their acoustic performance was evaluated using manual and automatic measurement methods.

Among the bonded foam samples, a coloured bonded foam with bitumen heavy layer and a polyurethane foam with heavy layer demonstrated the best acoustic performance. Results were surprising as the coloured foam had a relative low density compared to the other samples. As for the polyurethane foam, the good acoustic performance is related to its high density and greater thickness, specially when looking at the low frequency range sound transmission loss values. Geopolymers also showed promising results, particularly the samples with 30 mm and 40 mm thickness. The findings consistently supported the notion that materials with higher density and larger thickness offer superior sound insulation properties. The experimental procedure was improved by developing a sample holder to support the samples and allowing samples of various thicknesses to be tested. Additional components were also developed to enable the correct orientation of probe in relation to the sample plane and to allow its fixation to the 3D printer, which provided the mechanical manipulator of the automated sweeping system of the intensity probe. Other requirements such as constant scanning speed and the correct distance between sample and probe were also fulfilled.

Scan & Paint measurements were performed and provided detailed sound intensity data for each frequency of each sample, enabling the calculation of sound transmission loss using the pressure-intensity method as indicated in the ISO 15186-1 standard. Sound maps regarding sound intensity were generally uniform across most frequencies, except in the low-frequency range in the tests conducted with the automated system. This discrepancy in the low frequency range suggests that the automatic measurements may have limitations in accurately capturing sound characteristics at lower frequencies.

Consequently, the differences in transmission loss between the manual and automatic measurement methods were substantial. The lack of a calibration factor to access the effect of the noise emitted by the automatic system and the non-existence of perfect or favourable anechoic conditions in the receiving side (hemi anechoic chamber) due to reflective nature of the components that were placed there, such as aluminium profiles, cables and other components, may have affected results and contributed to the great disparities in sound transmission loss when compared to the manual method.

Based on the results and the observed discrepancies, it is essential to question the reliability of the results obtained from the automatic measurements. Even though automatic tests offer advantages such as efficiency and greater repeatability, the discrepancies raise concerns about their accuracy and applicability in this specific context. Therefore, the best materials, as identified in the study, are those for which the results were obtained through manual testing, as they are supported by existing studies in the literature that prove their trustworthiness and are extensively used in industrial applications.

To conclude, tested bonded foams and geopolymers demonstrate favourable sound transmission loss properties, making them promising candidates for application in heat pump systems. By incorporating these materials into heat pump components, such as compressor jackets and refrigerant circuit insulation, it is possible to achieve effective noise reduction while improving energy efficiency and system performance.

7.3   Future work

While this study provided valuable insights into the acoustic performance of different materials for sound insulation in heat pumps, there are several possibilities for future research and improvements that can be made.

First and most importantly, despite the advantages of automated testing such as increased efficiency and repeatability, the disparities observed in the transmission loss results between manual and automatic measurements suggest the need for further investigation. Future work should focus on refining the automated testing procedure, including the scanning pattern and the positioning of the intensity probe, to ensure consistent and accurate measurements across all frequencies, especially in the low-frequency range. While the Scan & Paint measurements provided valuable sound intensity results for each frequency, future studies could consider incorporating additional measurement techniques for a comprehensive analysis. Moreover, if further tests are to be made using an automated scanning system such as the one presented in this work, a calibration factor to incorporate into the sound transmission loss calculation formula is crucial to promote the reliability of these results and should be the main objective to pursue.

The development of a sample holder to support the samples was a valuable improvement in the experimental procedure. However, it would be beneficial to explore different sample holder designs to optimize sample stability during testing. Additionally, the influence of sample holder materials on the overall sound transmission loss should be investigated to evaluate potential acoustic leakage or interference. In this work, MDF was used.

Since the small scale reverberation chamber had problems regarding diffusivity in the 200 Hz to 400 Hz frequency range, it would be beneficial to place some diffusers to enhance sound pressure level uniformity in that specific range [22].

As for materials, the focus was on bonded foam samples, geopolymer samples, and their variations in thickness and density. As stated before, results were quite promising, but there is a wide range of other materials available for sound insulation purposes. Future investigation could involve testing and evaluating alternative materials, such as composite structures, porous materials, cork and wood panels, to identify potential candidates with superior acoustic performance for heat pump applications. Moreover, exploring different sample configurations, such as multilayer assemblies or the integration of sound-absorbing materials, could provide insights into enhanced sound insulation solutions.

This study highlighted the importance of density and thickness in determining the acoustic performance of the materials. Nevertheless, it would also be interesting to tests these same materials in greater number and with various thicknesses to more accurately access their effect on sound transmission loss.

In addition to acoustic performance, the cost-effectiveness of sound insulation materials is an important consideration for industrial applications. An extra suggestion would be to perform a comprehensive cost analysis, taking into account not only the material cost but also installation expenses, maintenance requirements, and expected lifespan. This analysis would assist in identifying materials that offer the best balance between acoustic performance and cost efficiency.

Lastly, with increasing concern on sustainable practices, future work could focus on a life cycle analysis to quantify the environmental footprint of different materials, considering factors such as raw material extraction, manufacturing processes and end-of-life.

References

[1] Bosch, "Bosch Aveiro." `https://www.bosch.pt/a-nossa-empresa/bosch-em-portugal/aveiro/`. Accessed on 13/02/2023.

[2] "Heat pump market size, share trends analysis report by technology (water source, air source, ground source), by application (commercial, residential, industrial), by region, and segment forecasts, 2022 - 2030," tech. rep., Grand View Report.

[3] Reuters, "The Important Role of Heat Pumps in a Sustainable Future." `https://www.reuters.com/article/sponsored/the-important-role-of-heat-pumps-in-a-sustainable-future`. Accessed on 15/02/2023.

[4] I. Staffell, D. Brett, N. Brandon, and A. Hawkes, "A review of domestic heat pumps," *Energy & Environmental Science*, vol. 5, no. 11, pp. 9291–9306, 2012.

[5] EHPA, "Types of heat pumps." `https://www.ehpa.org/about-heat-pumps/types-of-heat-pumps/`. Accessed on 16/02/2023.

[6] S. Wagner, X. Carniel, J. Rohlfing, K. Bay, and H. Hellgren, "Overview on Heat Pump Component Noise and Noise Control Techniques." `https://heatpumpingtechnologies.org/annex51/wp-content/uploads/sites/59/2021/10/iea-hpt-annex-51-d3.pdf`, 2020. Accessed on 16/02/2023.

[7] P. Carroll, M. Chesser, and P. Lyons, "Air source heat pumps field studies: A systematic literature review," *Renewable and sustainable energy reviews*, vol. 134, p. 110275, 2020.

[8] B. Berglund, T. Lindvall, D. H. Schwela, *et al.*, "Guidelines for community noise," 1999.

[9] G. D. of Energy Climate Change, "Acoustic Noise Measurements of Air Source Heat Pumps." `https://www.gov.uk/government/publications/acoustic-noise-measurements-of-air-source-heat-pumps`, 2011. Accessed on 17/02/2023.

[10] R. Fumagalli, P. Wagner, *et al.*, "IEA Heat Pumping Technologies." `https://heatpumpingtechnologies.org/annex51/wp-content/uploads/sites/59/2021/10/iea-hpt-annex-51-d12.pdf`, 2020. Accessed on 17/02/2023.

[11] Siemens, "Sound Transmission Loss." `https://community.sw.siemens.com/s/article/sound-transmission-loss`, October 2019. Accessed on 26/02/2023.

[12] K. Ghorbani, H. Hasani, M. Zarrebini, and R. Saghafi, "An investigation into sound transmission loss by polypropylene needle-punched nonwovens," *Alexandria Engineering Journal*, vol. 55, no. 2, pp. 907–914, 2016.

[13] R. M. Novais, J. Carvalheiras, L. Senff, A. M. Lacasta, I. R. Cantalapiedra, J. Giro-Paloma, M. P. Seabra, and J. A. Labrincha, "Multifunctional cork–alkali-activated fly ash composites: A sustainable material to enhance buildings' energy and acoustic performance," *Energy and Buildings*, vol. 210, p. 109739, 2020.

[14] "ISO 10140-1:2021 Acoustics — Laboratory measurement of sound insulation of building elements — Part 1: Application rules for specific products." `https://www.iso.org/obp/ui/#iso:std:iso:10140:-1:ed-3:v1:en`. Accessed on 01/03/2023.

[15] "ISO 15186-1:2000 Acoustics — Measurement of sound insulation in buildings and of building elements using sound intensity — Part 1: Laboratory measurements." `https://www.iso.org/standard/26097.html`. Accessed on 01/03/2023.

[16] M. Cassidy, R. K. Cooper, R. Gault, and J. Wang, "Evaluation of standards for transmission loss tests," *Journal of the Acoustical Society of America*, vol. 123, no. 5, p. 3190, 2008.

[17] M. Viscardi and P. Napolitano, "Numerical prediction and experimental validation of sound transmission loss for sandwich panels," *Computer and Mathematics in Automation and Materials Science*, vol. 22, pp. 117–22, 2014.

[18] Z. Luo, T. Li, Y. Yan, Z. Zhou, and G. Zha, "Prediction of sound insulation performance of aramid honeycomb sandwich panel based on artificial neural network," *Applied Acoustics*, vol. 190, p. 108656, 2022.

[19] R. del Rey, J. Alba, J. C. Rodríguez, and L. Bertó, "Characterization of new sustainable acoustic solutions in a reduced sized transmission chamber," *Buildings*, vol. 9, no. 3, p. 60, 2019.

[20] W.-H. Tan, E. Lim, H. Chuah, E. Cheng, and C. Lam, "Sound transmission loss of natural fiber panel," *International Journal of Mechanical & Mechatronics Engineering*, vol. 16, no. 6, pp. 33–42, 2016.

[21] E. Piollet, M.-A. Bianki, and A. Ross, "A mobile reverberation cabin for acoustic measurements in an existing anechoic room," in *INTER-NOISE and NOISE-CON Congress and Conference Proceedings*, vol. 253, pp. 2931–2942, Institute of Noise Control Engineering, 2016.

[22] L.-g. Wang, Q. Zhang, X.-r. Qin, and Y.-t. Sun, "Design of a small reverberation box based on bem-sea method," *Journal of Vibroengineering*, vol. 17, no. 4, pp. 1707–1718, 2015.

[23] D. F. Comesana, E. Tijs, and H.-E. de Bree, "Exploring the properties of acoustic particle velocity sensors for near-field noise source localisation applications," in *Forum Acusticum*, September 2014.

[24] D. Fernandez Comesaña, S. Steltenpool, G. Pousa, H.-E. Bree, and K. Holland, "Scan and paint: Theory and practice of a sound field visualization method," *ISRN Mechanical Engineering*, vol. 2013, 01 2013.

[25] D. F. Comesaña, S. Steltenpool, M. Korbasiewicz, and E. Tijs, "Direct acoustic vector field mapping: new scanning tools for measuring 3d sound intensity in 3d space," in *Proc. Euronoise*, pp. 891–895, 2015.

[26] D. F. Comesana, J. Wind, A. Grosso, and K. R. Holland, "Performance of p-p and p-u intensity probes using scan & paint," in *18th International Conference of Noise and Vibration*, July 2011.

[27] D. Siano, M. Viscardi, and M. Panza, "Experimental acoustic measurements in far field and near field conditions: characterization of a beauty engine cover," *Recent Advances in Fluid Mechanics and Thermal Engineering*, pp. 50–57, 2014.

[28] D. F. Comesana and S. Steltenpool, "Mapping stationary sound fields using scanning techniques the fundamentals of scan & paint," in *20th International Congress on Sound and Vibration (ICSV20)*, July 2013.

[29] M. Guiot, D. Fernandez Comesaña, M. Korbasiewicz, and G. Pousa, "Turbo-compressor and piping noise assessment using a particle velocity based sound emission method," in *Proceedings of the INTER-NOISE and NOISE-CON Congress and Conference Proceedings, Dubrovnik, Croatia*, pp. 9–12, 2015.

[30] R. Del Rey, J. Alba, J. P. Arenas, and V. J. Sanchis, "An empirical modelling of porous sound absorbing materials made of recycled foam," *Applied Acoustics*, vol. 73, no. 6, pp. 604–609, 2012.

[31] B. Mohammadi, A. Safaiyan, P. Habibi, and G. Moradi, "Evaluation of the acoustic performance of polyurethane foams embedded with rock wool fibers at low-frequency range; design and construction," *Applied Acoustics*, vol. 182, no. 108223, 2021.

[32] Y. Tao, M. Ren, H. Zhang, and T. Peijs, "Recent progress in acoustic materials and noise control strategies–a review," *Applied Materials Today*, vol. 24, no. 101141, 2021.

[33] R. M. Novais, R. C. Pullar, and J. A. Labrincha, "Geopolymer foams: An overview of recent advancements," *Progress in Materials Science*, vol. 109, no. 100621, 2020.

[34] R. Maderuelo-Sanz, A. V. Nadal-Gisbert, J. E. Crespo-Amorós, J. M. B. Morillas, F. Parres-García, and E. J. Sanchis, "Influence of the microstructure in the acoustical performance of consolidated lightweight granular materials," *Acoustics Australia*, vol. 44, pp. 149–157, 2016.

[35] C. Leiva, Y. Luna-Galiano, C. Arenas, B. Alonso-Fariñas, and C. Fernández-Pereira, "A porous geopolymer based on aluminum-waste with acoustic properties," *Waste Management*, vol. 95, pp. 504–512, 2019.

[36] Z. Zhang, J. L. Provis, A. Reid, and H. Wang, "Mechanical, thermal insulation, thermal resistance and acoustic absorption properties of geopolymer foam concrete," *Cement and Concrete Composites*, vol. 62, pp. 97–105, 2015.
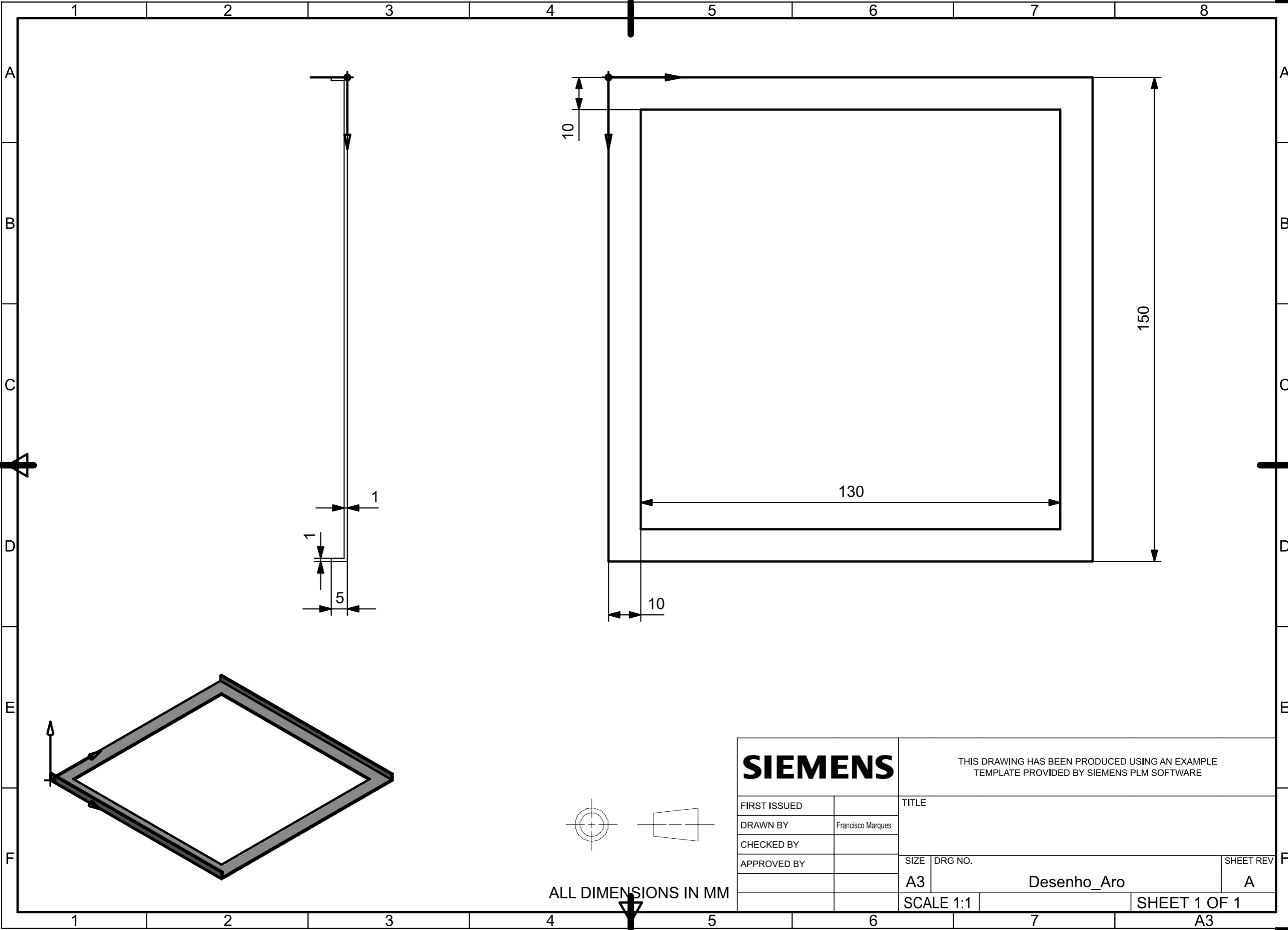
[37] X. Liu, C. Hu, and L. Chu, "Microstructure, compressive strength and sound insulation property of fly ash-based geopolymeric foams with silica fume as foaming agent," *Materials*, vol. 13, no. 14, p. 3215, 2020.

[38] I. Perna, T. Hanzlicek, P. Straka, and M. Steinerova, "Acoustic absorption of geopolymer/sand mixture," *Ceramics–Silikáty*, vol. 53, no. 1, pp. 48–51, 2009.

[39] M. A. Villaquirán, V. N. Perea, J. E. Ruiz, and R. M. de Gutiérrez, "Mechanical, physical and thermoacoustic properties of lightweight composite geopolymers," *Ingeniería y competitividad: revista científica y tecnológica*, vol. 24, no. 1, p. 8, 2022.

[40] R. M. Novais, L. Senff, J. Carvalheiras, A. M. Lacasta, I. R. Cantalapiedra, and J. A. Labrincha, "Simple and effective route to tailor the thermal, acoustic and hygrothermal properties of cork-containing waste derived inorganic polymer composites," *Journal of Building Engineering*, vol. 42, no. 102501, 2021.

[41] Naturally:wood, "Wood's acoustic properties ." `https://www.naturallywood.com/wood-performance/acoustic/`. Accessed on 18/03/2023.

[42] E. Sokol, "Does Wood Absorb or Reflect Sound? ." `https://bettersoundproofing.com/does-wood-absorb-or-reflect-sound/#Sound_Absorption`, May 2022. Accessed on 19/04/2023.

[43] A. L. Neto, J. R. M. da Silva, J. T. Lima, and G. F. Rabelo, "Efeito das diferentes madeiras no isolamento acústico," *Floresta*, vol. 38, no. 4, 2008.

[44] A. Santoni, P. Bonfiglio, P. Fausti, C. Marescotti, V. Mazzanti, and F. Pompoli, "Characterization and vibro-acoustic modeling of wood composite panels," *Materials*, vol. 13, no. 8, p. 1897, 2020.

[45] F. A. Everest and K. C. Pohlmann, *Master handbook of acoustics.* McGraw-Hill Education, 2022.

[46] A. D. Pierce and A. Acoustics, "Introduction to its physical principles and applications," *Acoustical Society of America and American Institute of Physics*, p. 122, 1981.

[47] C. H. Hansen, "Fundamentals of acoustics," *Occupational Exposure to Noise: Evaluation, Prevention and Control. World Health Organization*, vol. 1, no. 3, pp. 23–52, 2001.

[48] C. Sujatha, *Vibration, Acoustics and Strain Measurement: Theory and Experiments.* Springer Nature, 2023.

[49] J. P. Guyer and R. PE, "Fundamentals of acoustics," *Continuing Education and Development, Inc Course*, no. M02-022, p. 31, 2009.

[50] "ISO 18405:2022 Underwater acoustics — Terminology ." `https://www.iso.org/obp/ui/#iso:std:iso:18405:ed-1:v1:en`. Accessed on 21/04/2023.

[51] L. L. Beranek and T. Mellow, *Acoustics: sound fields and transducers*. Academic Press, 2012.

[52] G. M. Smith, "Sound and Noise Measurement with Microphone Transducers." `https://dewesoft.com/blog/sound-measurement-with-microphone-sensors`, January 2022. Accessed on 01/06/2023.

[53] F. Jacobsen and H.-E. de Bree, "A comparison of two different sound intensity measurement principles," *The Journal of the Acoustical Society of America*, vol. 118, no. 3, pp. 1510–1517, 2005.

[54] Creality, "Ender 3 Classic DIY 3D Printer Best-Value-For-Money." `https://www.creality.com/products/ender-3-3d-printer?spm=..page_1967279.products_display_1.1&spm_prev=..product_ce00868d-efe2-4fa8-9168-240e7c3b3cd1.header_1.1`. Accessed on 06/05/2023.

[55] Recticel, "Bonded foam." `https://recticelflexiblefoams.com/sportsleisure/about-us/our-expertise/our-technologies/bonded-foam.html`. Accessed on 07/05/2023.

[56] C. Zhang, J. Li, Z. Hu, F. Zhu, and Y. Huang, "Correlation between the acoustic and porous cell morphology of polyurethane foam: Effect of interconnected porosity," *Materials & Design*, vol. 41, pp. 319–325, 2012.

[57] Norsonic, "Reference Sound Source Nor278." `https://web2.norsonic.com/product_single/reference-sound-source-nor278/`. Accessed on 27/03/2023.

[58] HEADacoustics, "ArtemiS SUITE – Software platform for sound and vibration analyses." `https://www.head-acoustics.com/products/analysis-software/artemis-suite`. Accessed on 27/03/2023.

[59] Microflown, "Software — Velo." `https://www.microflown.com/products/software`. Accessed on 27/03/2023.

Intentionally blank page.

Appendix A

Technical drawings

ALL DIMENSIONS IN MM

1

1

5

10

150

130

10

SIEMENS

		TITLE		
FIRST ISSUED				
DRAWN BY	Francisco Marques			
CHECKED BY				
APPROVED BY				
		SIZE	DRG NO.		SHEET REV
		A3	Desenho_Aro		A
		SCALE 1:1		SHEET 1 OF 1	

A3

290

A

4 x M6 - ∅ 6 Custom THRU

400

70

130

150

10

125

10

10

15

5

10

SECTION A-A

A

SIEMENS

FIRST ISSUED		TITLE			
DRAWN BY	Francisco Marques				
CHECKED BY					
APPROVED BY		SIZE	DRG NO.		SHEET REV
		A3	Cover_Plate		A
		SCALE 1:3		SHEET 1 OF 1	

ALL DIMENSIONS IN MM

SECTION A-A

A

A

25
20
40
5
10
130
150
10

290
20
80
400
135
20
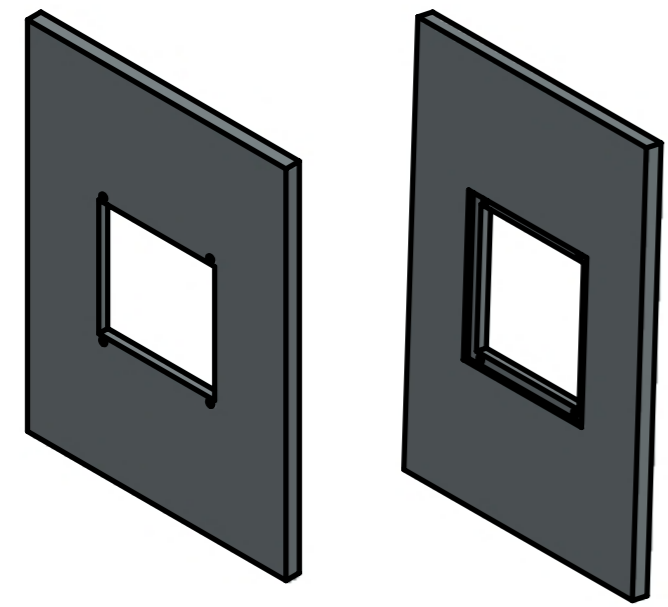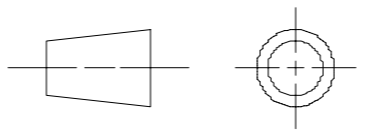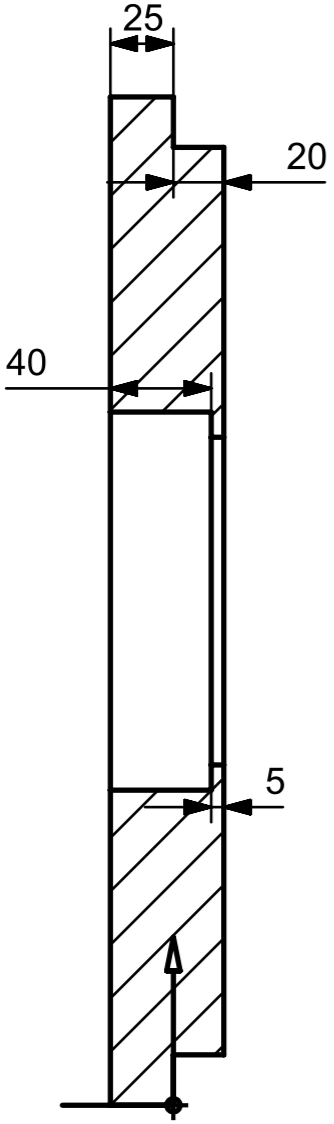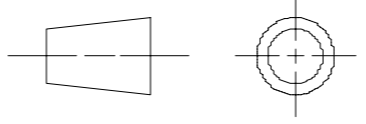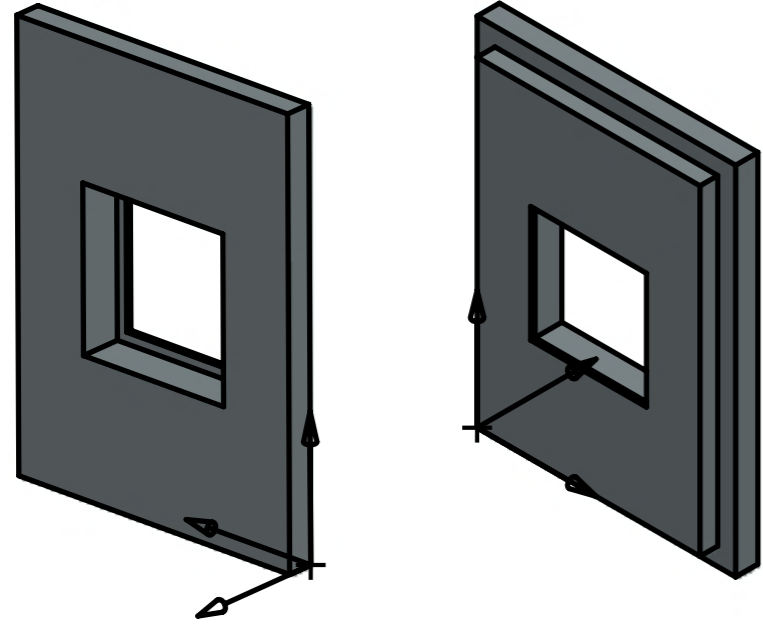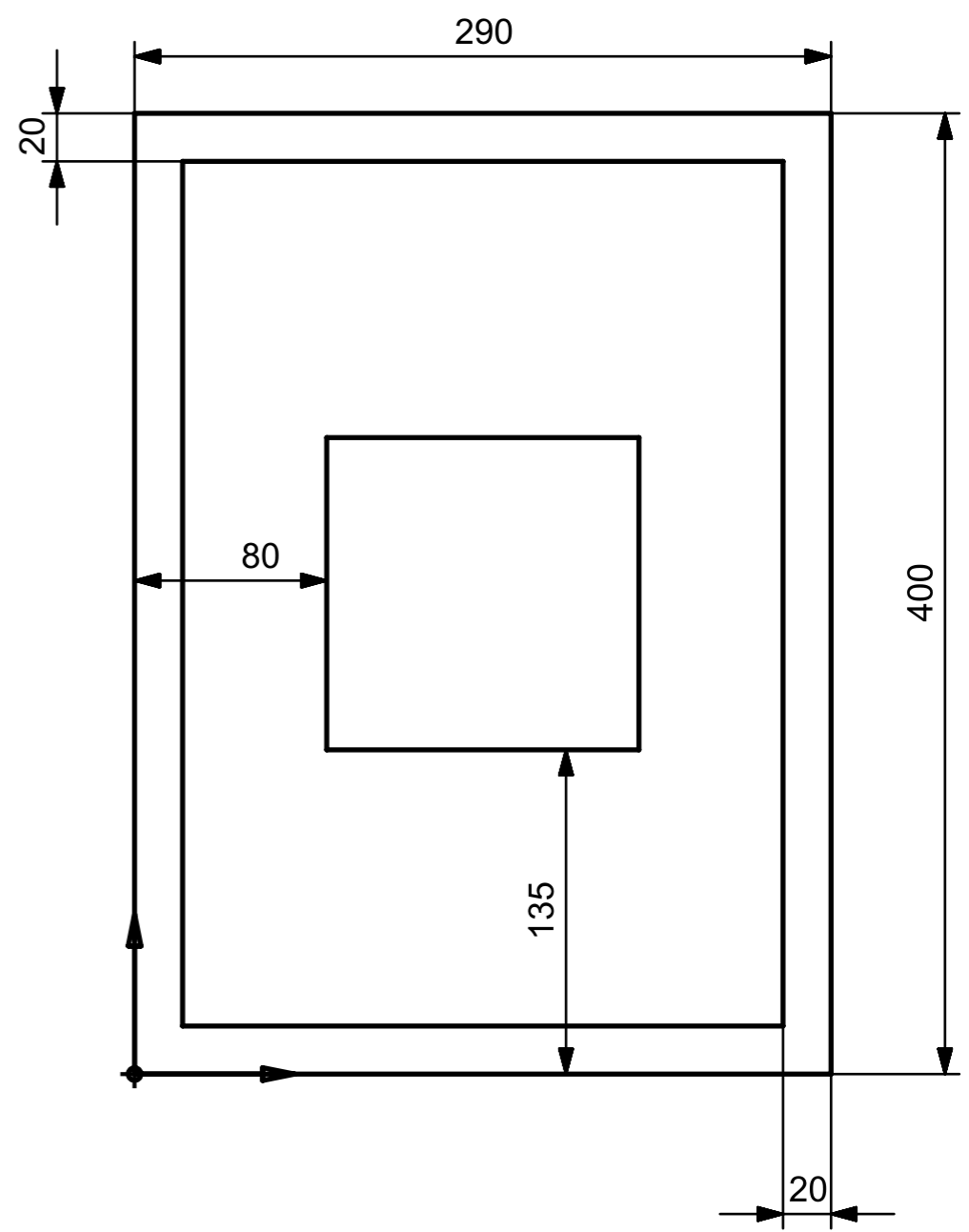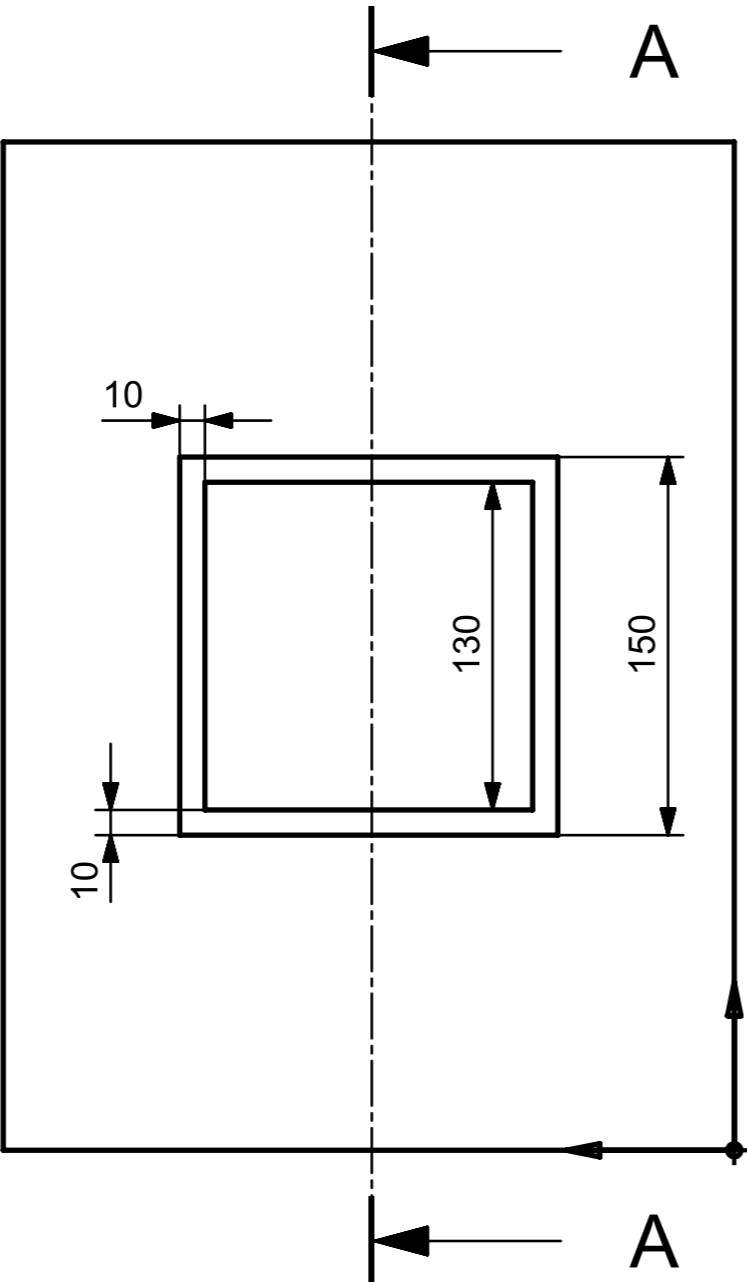
ALL DIMENSIONS IN MM

SIEMENS

FIRST ISSUED		TITLE			
DRAWN BY	Francisco Marques				
CHECKED BY					
APPROVED BY		SIZE	DRG NO.		SHEET REV
		A3		MotherPlate	A
		SCALE 1:3			SHEET 1 OF 1

Top view dimensions: 25,50 · 3,20 · 3,00 · 3,00 · 10,00

Front view dimensions: 31,50 · 54,00 · 20,00 · R10,00 · 28,50 · R4,00 · R4,00 · 24,00 · 2,12 · 2,12 · 2,12 · 2,12 · 9,50 · 29,00 · 9,50 · 8,00 · 8,00

A — A (Section line)

Bottom view dimensions: 3,75 · 70,00 · 3,00 · 64,00 · 2,50

SECTION A-A
Dimensions: 30,00 · 21,00 · 9,00
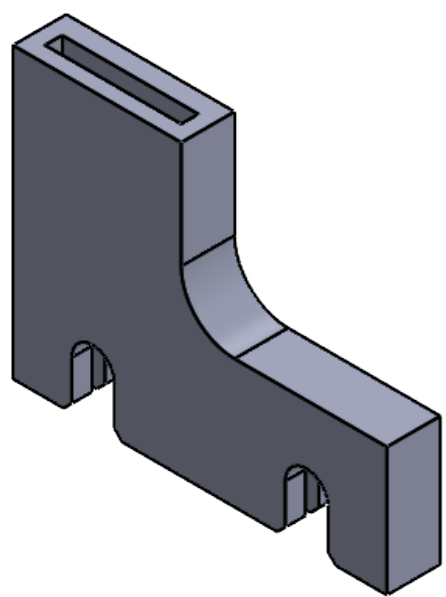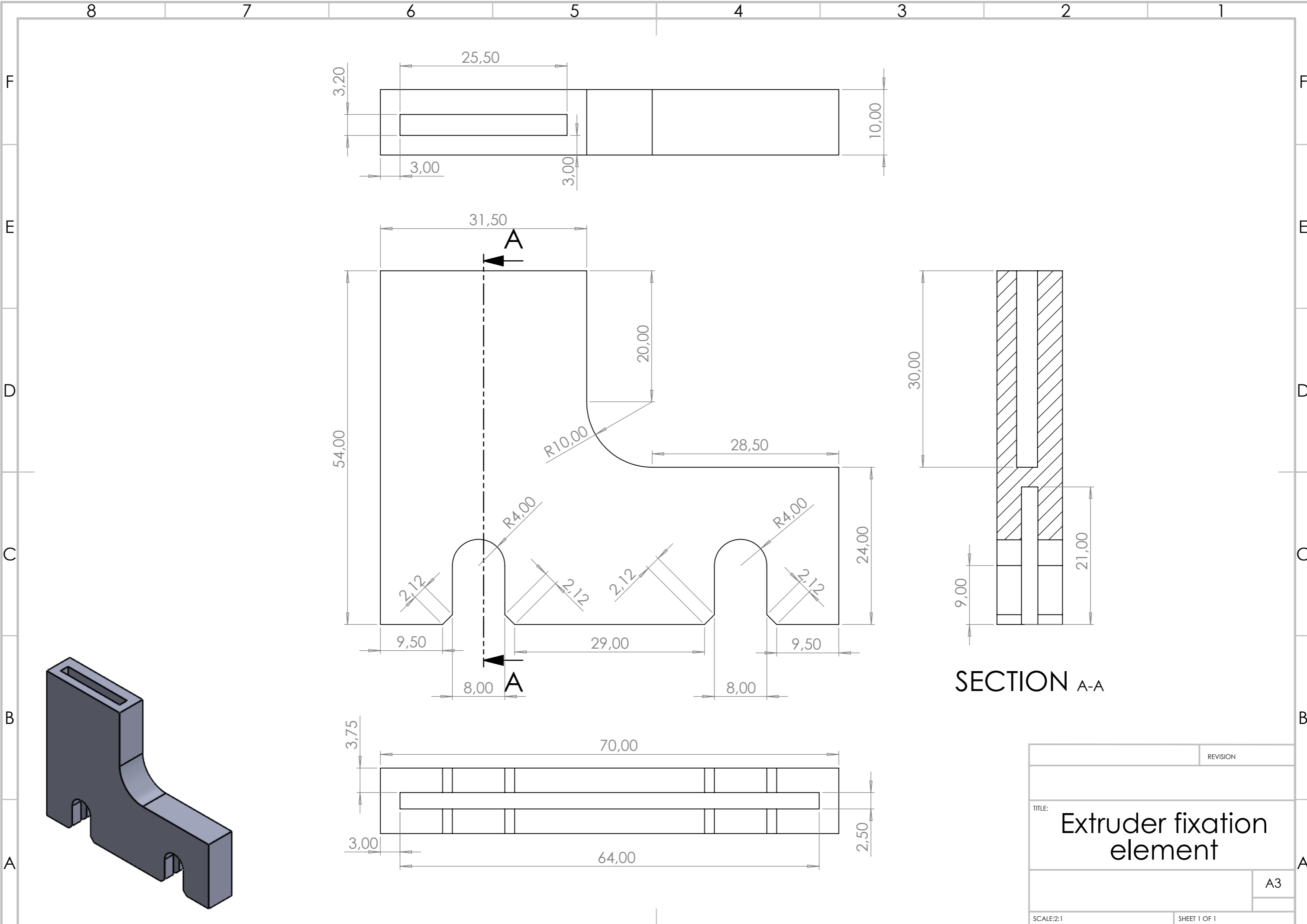
TITLE:	REVISION
Extruder fixation element	
	A3

SCALE:2:1 SHEET 1 OF 1

C

3,00

R6,35

R5,00

R5,00

20,00

4,00

35,00

10,00

C

32,00

9,35

25,50

11,00

60,35

32,00

SECTION C-C

SCALE 2 : 1

3,20

3,25

3,40

TITLE:

Probe support

A3

SCALE:1:1

SHEET 1 OF 1
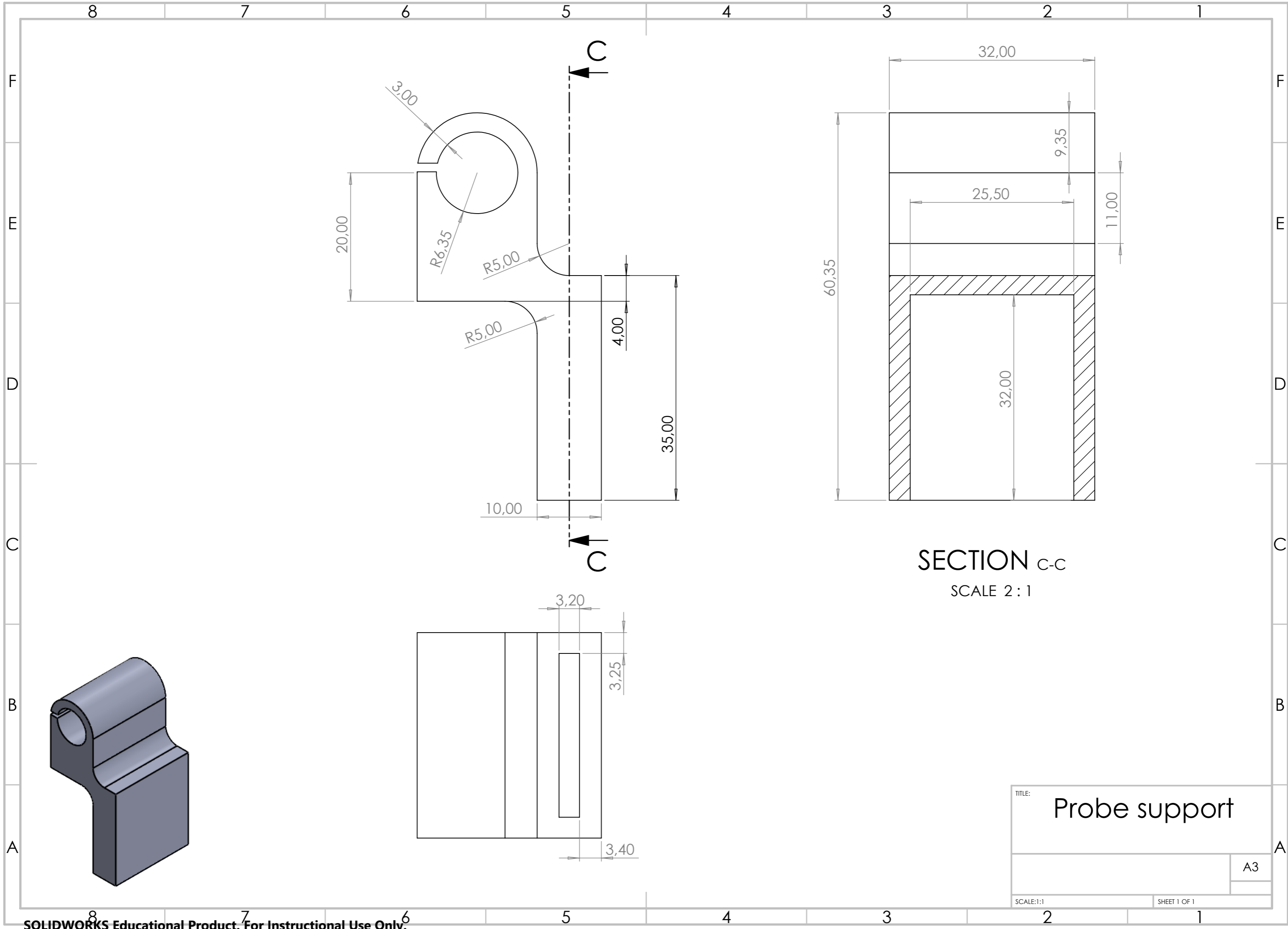
Appendix B

Python script for data treatment

```python
import pandas as pd
import os
from tkinter import Tk
from tkinter.fildedialog import ask directory
import warnings
import subprocess

Tk().withdraw()
print('Choose Folder')
mainfolder_path = askdirectory(title='Choose Main Folder')
data_folders=next(os.walk(mainfolder_path))[1]
print('-------File Chosen------')
result_path = mainfolder_path + '/Overall.xlsx'

count = 0
for current in data_folders:
    print('Analysing ' + current)
    count = count + 1
    organized_list = []
    averages = []
    folder_path = os.path.join(mainfolder_path, current)

    for filename in os.listdir(folder_path):
    filename = filename[0:filename.find('H')]
    organized_list.append(int(filename))
    organized_list.sort()
    organized_list_extended = str[(i) + 'Hz.xlsx' for i in organized_list
    ]
    folder_path=folder_path.replace('/','\\')

for filename in organized_list_extended:
    full_path = folder_path + '\\' + filename
    df = pd.read_excel(full_path, skiprows=rang(0,7), sheet_name='Data',
    engine='openpyxl', header = None
    avg = df.mean().mean()
    averages.append(avg)

df_avg = pd.DataFrame({"Frequency [Hz]": organized_list , "Avg. Sound
    Intesity [dB]": averages})
if count == 1:
    with pd.ExcelWriter(result_path) as writer:
        df_avg.to_excel(writer, sheet_name = current, index = False)
```

```
40 else:
41     with pd.ExcelWriter(result_path, mode = 'a') as writer:
42         df_avg.to_excel(writer, sheet_name = current, index = False)
43
44 print('-----Analysis done-----')
45 print('Done')
46 subprocess.Popen(r'explorer /select,'+ result_path.replace('/','\\'))
```